National Research Centre ”Kurchatov Institute”

Status and perspectives of proton irradiation tests at NRC KI

Alexander Ryazanov

29 April 2016, Malta, Italy

Cyclotron of NRC “Kurchatov Institute”

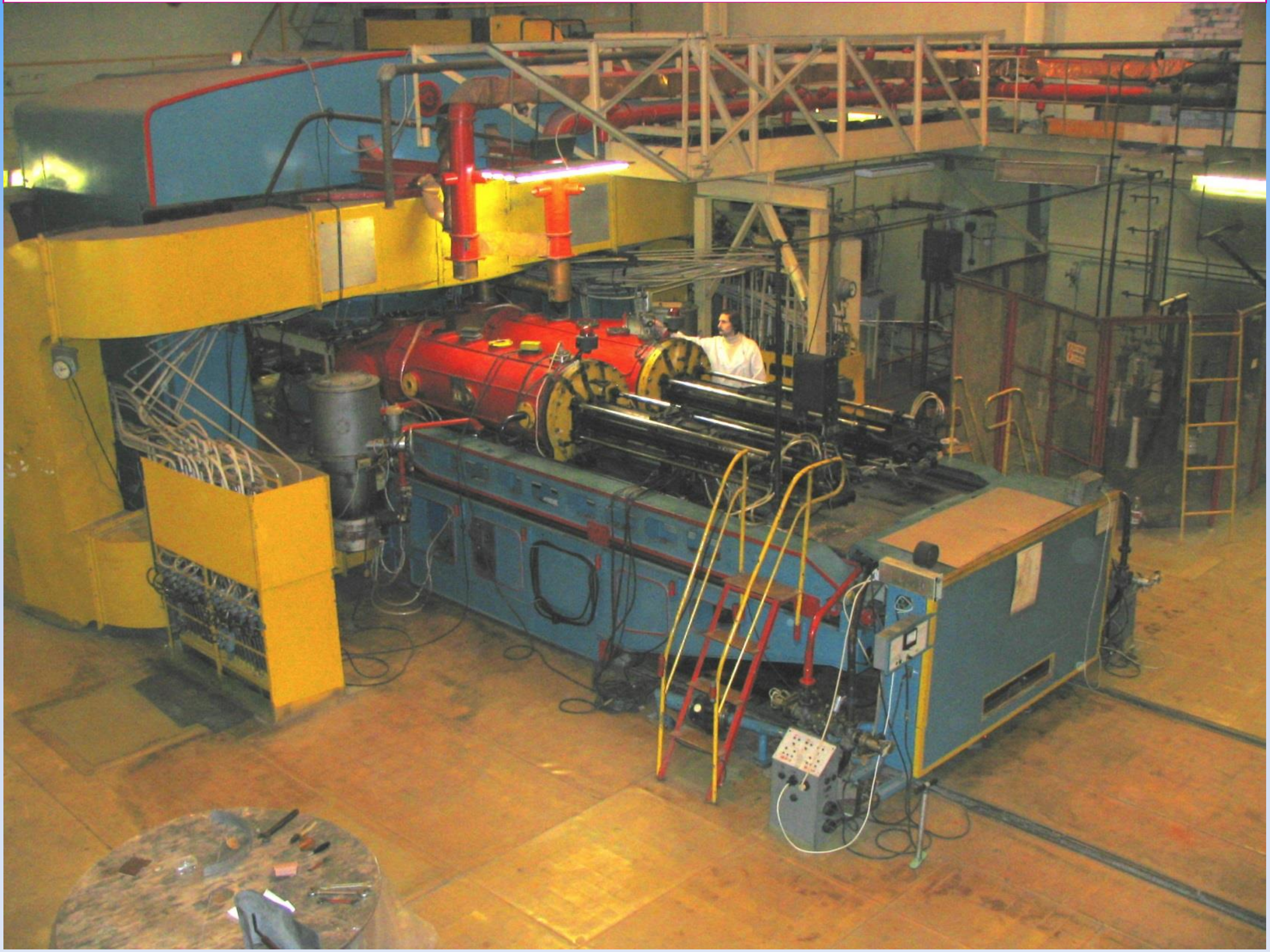

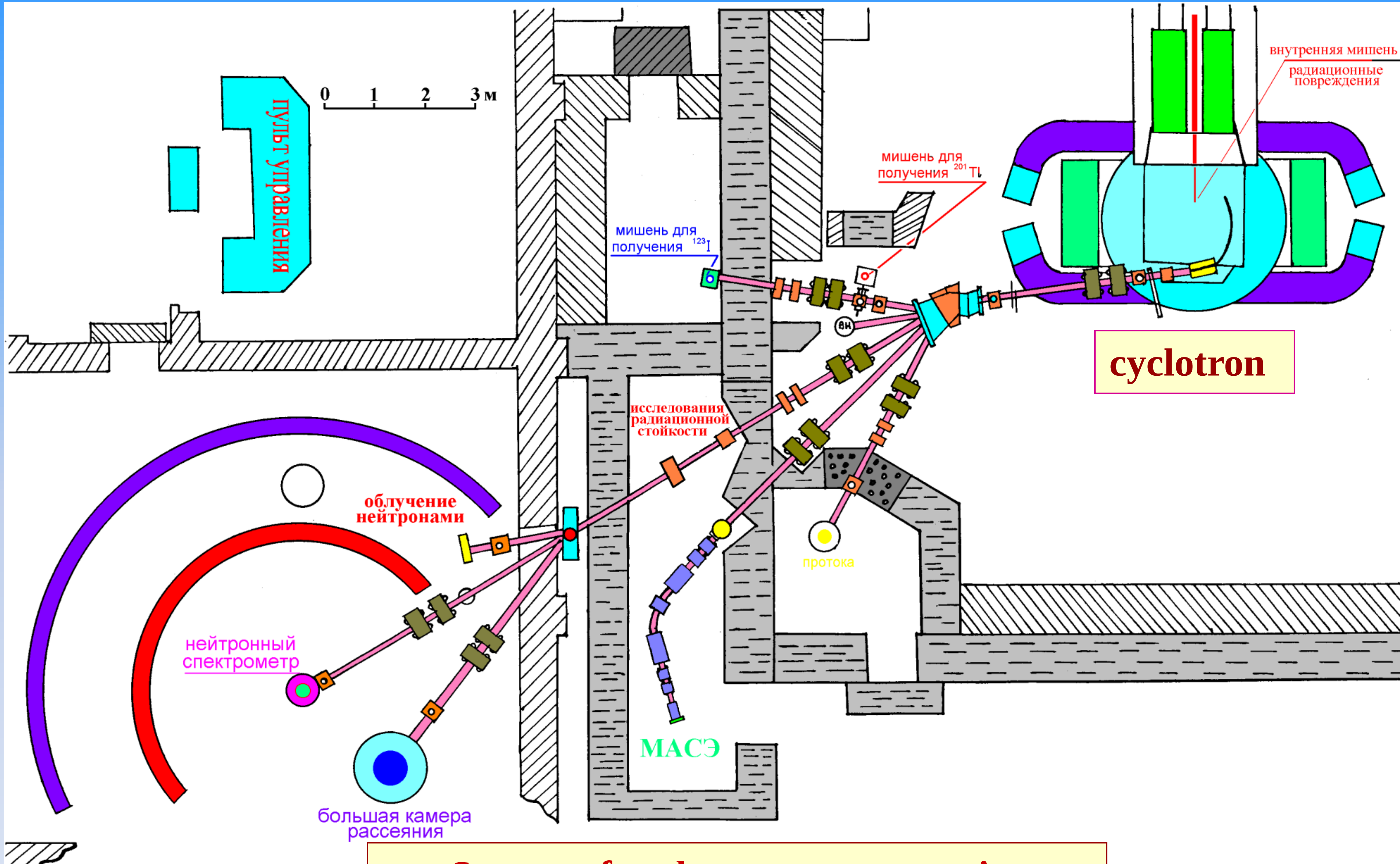

System of cyclotron transportation

Acceleration of Charged Particles on Cyclotron of National Research Centre “Kurchatov Institute”

- **Cyclotron of NRC KI:**

Protons with energy < 35 MeV, current J < 30 mkA

Helium ions He^4 with energy < 60 MeV, current J < 20 mkA

Ions O^{16} with energy < 120 MeV, current J < 5 mkA

Ions C^{12} with energy < 80 MeV, current J < 5 mkA

Sample holders for fast particle irradiation on NRC KI cyclotron

Preliminary design of the target unit

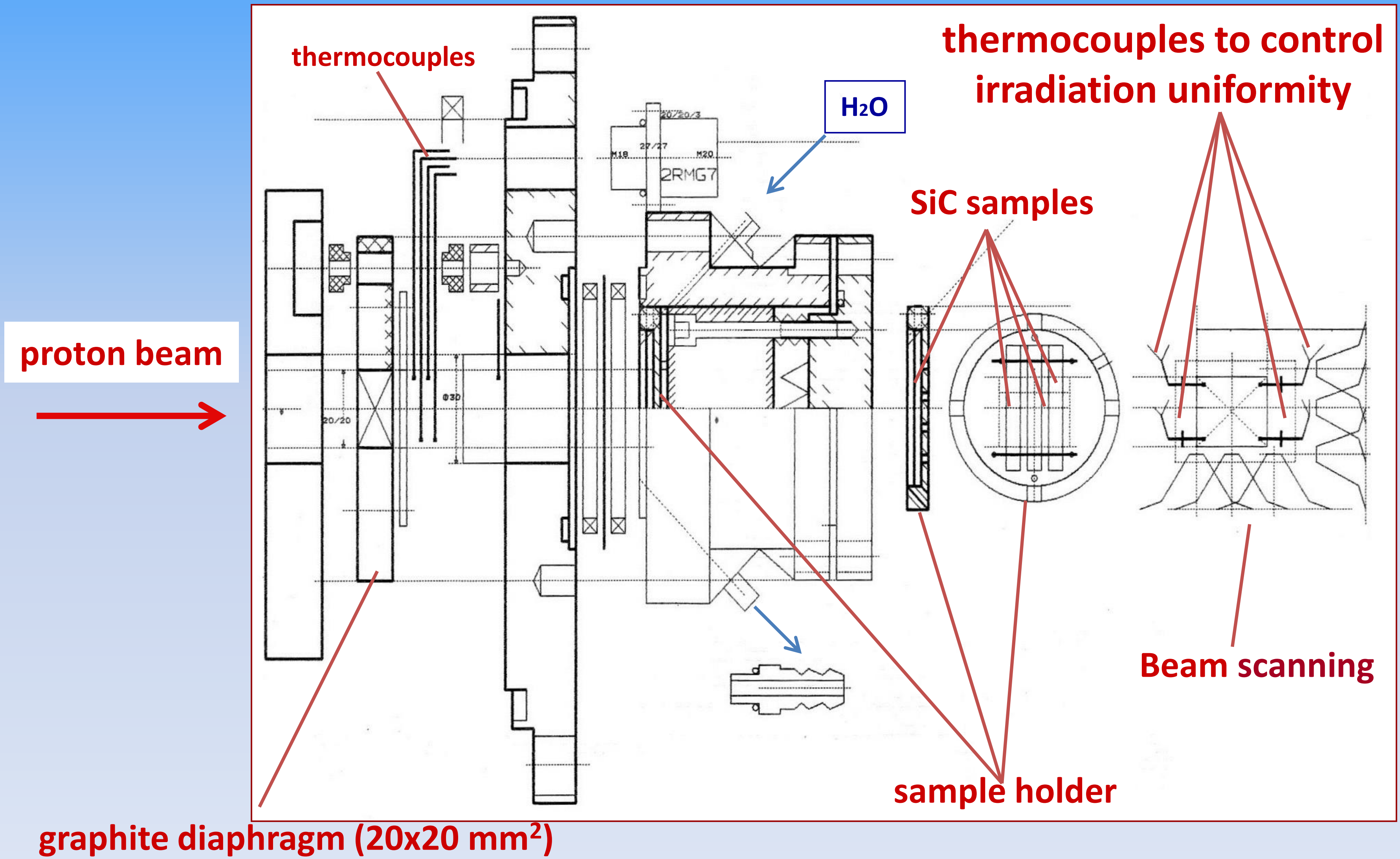

Schematic view of the target unit

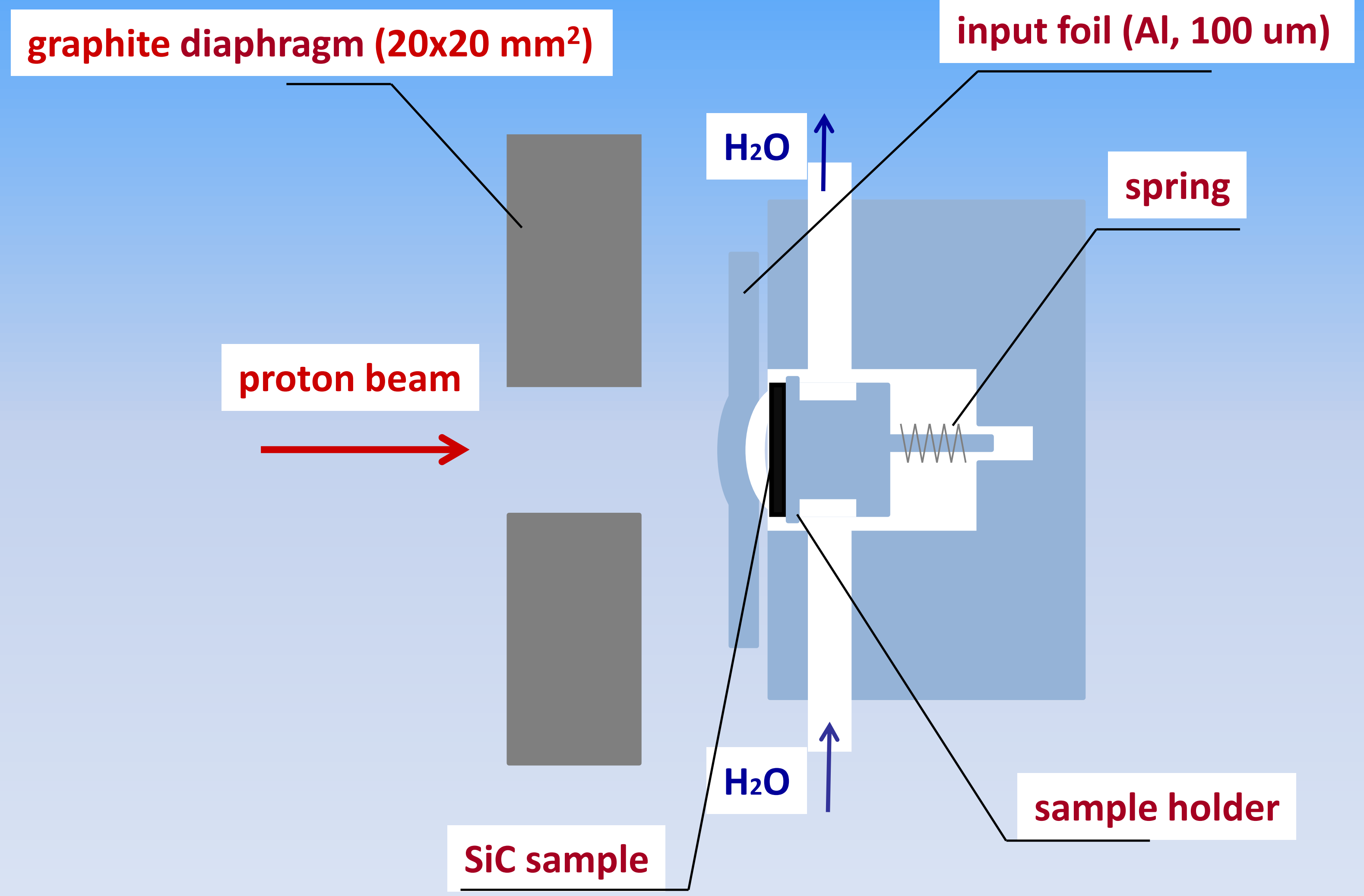

Front view of the sample holder

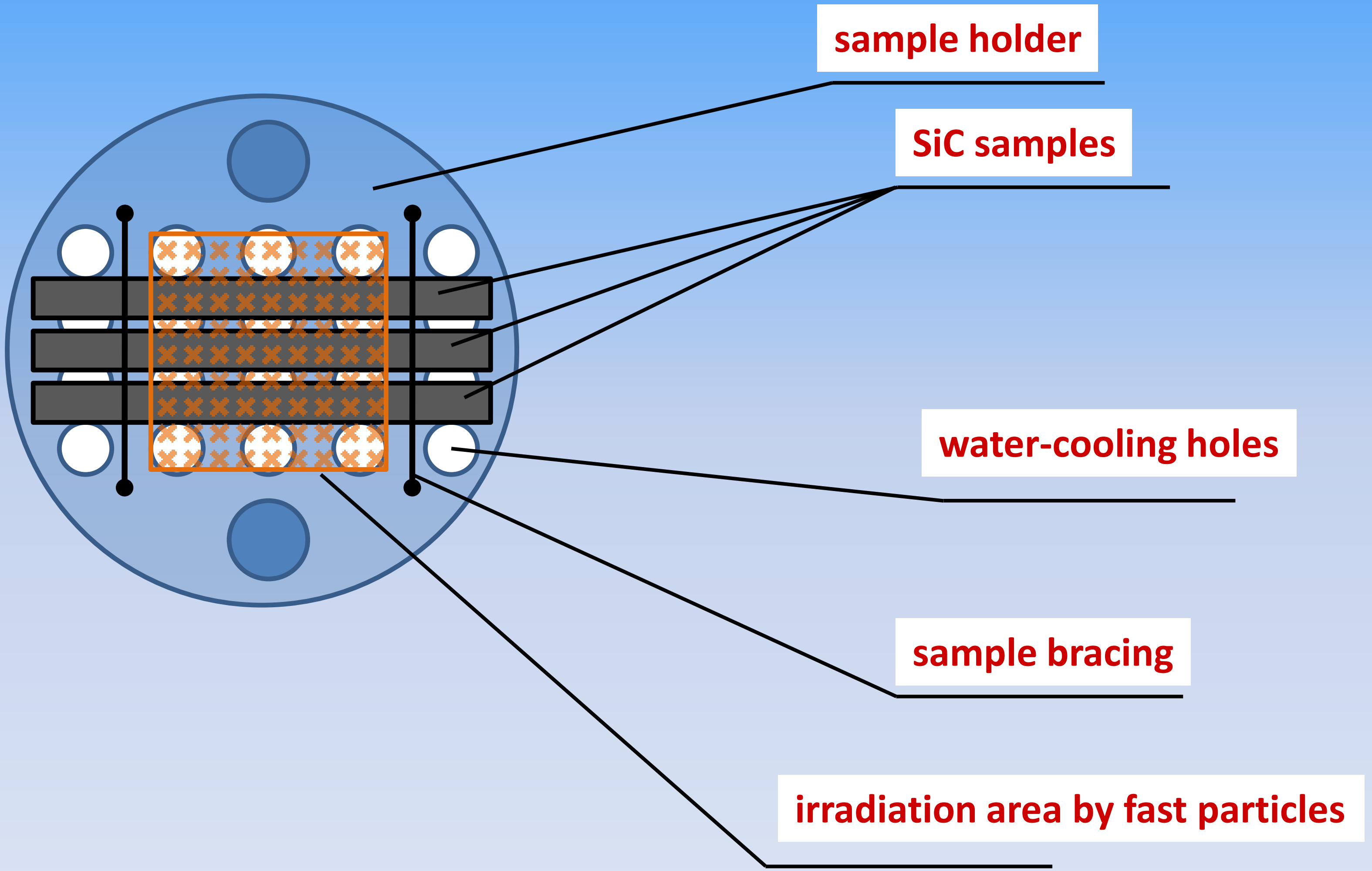

Investigations of initial microstructure of SiC before fast proton irradiation on NRC KI cyclotron

Microscopy and sample preparation

- **TEM:** **TITAN 80-300 (FEI, US) equipped with Cs probe-corrector (CEOS Germany), GIF (GATAN, US) and EDS (EDAX, US) at 300 kV.**

- **Preparation technique for samples.**

2 techniques were explored:

- **A. Mechanical thinning and polishing to 50-70 μm followed by Ar^+ milling in GATAN PIPS (GATAN, US) at 5 kV with 0.2 kV in final step.**
- **B. FIB etching in HELIOS (FEI, US) with Ga^+ at 30 kV followed by 2 kV at final step.**

Fabrication of SiC

SiC ***was first synthesized in 1891 by Acheson:***

(E.G.Acheson, Chem.News 68 (1893) 179).

By electrochemical reaction in an electric furnace:

$$SiO_2 + 3C \rightarrow SiC + 2CO$$

α-SiC formed at T = 2373 K and

β-SiC formed at T = 1273 – 1873 K

Examples of the crystal structure of SiC polytypes: 3C, 4H, 6H and 15R

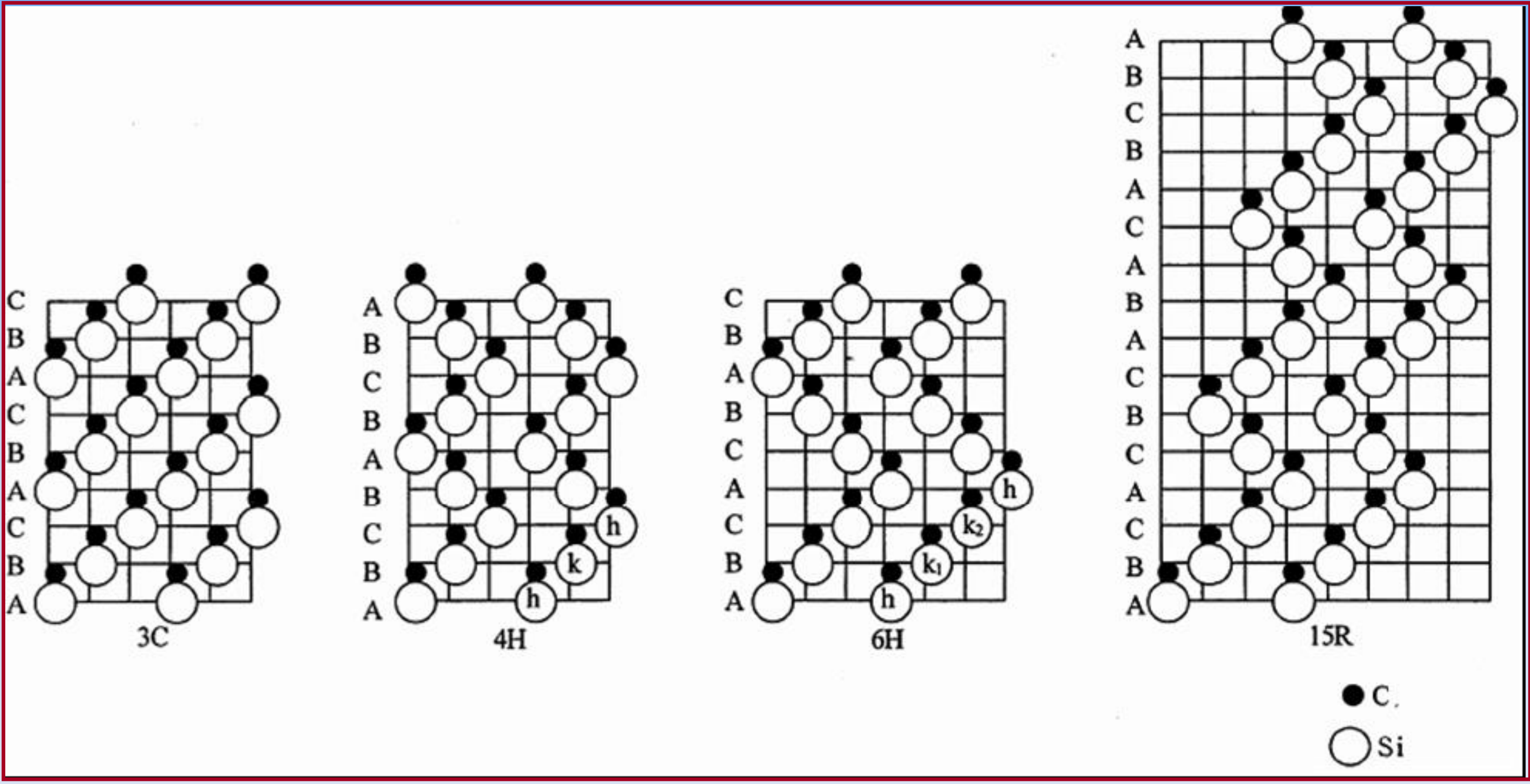

Phase stability diagram of SiC polytypes

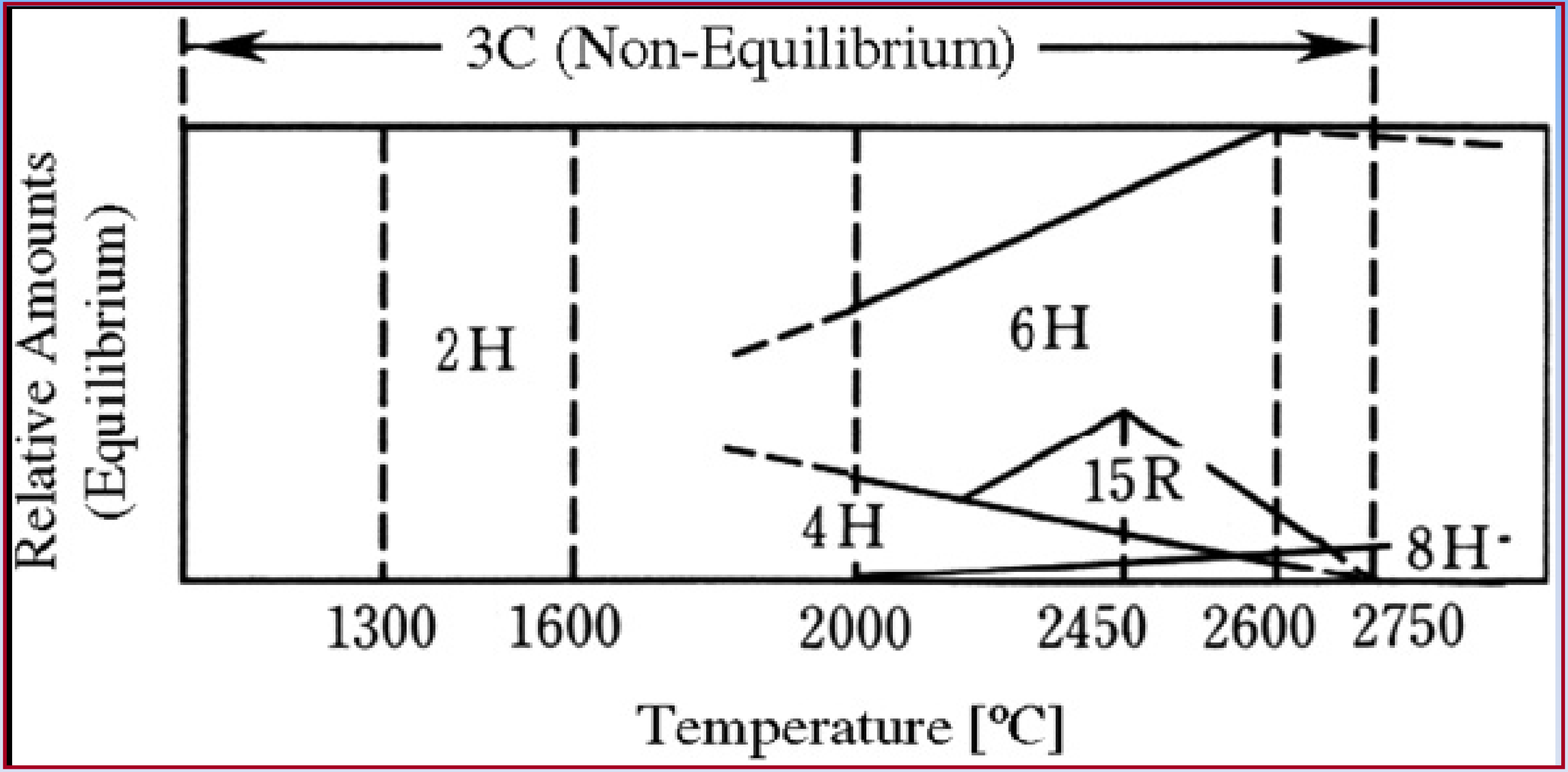

Lattice parameters and density of SiC polytypes at room temperature

Polytype	Density (g/cm3)	Lattice parameter (nm)
2H	3.219	a = 0.3081, c = 0.5031
3C	3.215	a = 0.43589
4H	3.215	a = 0.3081, c =1.0061
6H	3.215	a = 0.3081, c =1.5092
15R	–	a = 0.3073, c = 3.770
21R	–	a = 0.3073, c = 5.278

Crystal structures of (a) α-SiC and (b) β-SiC

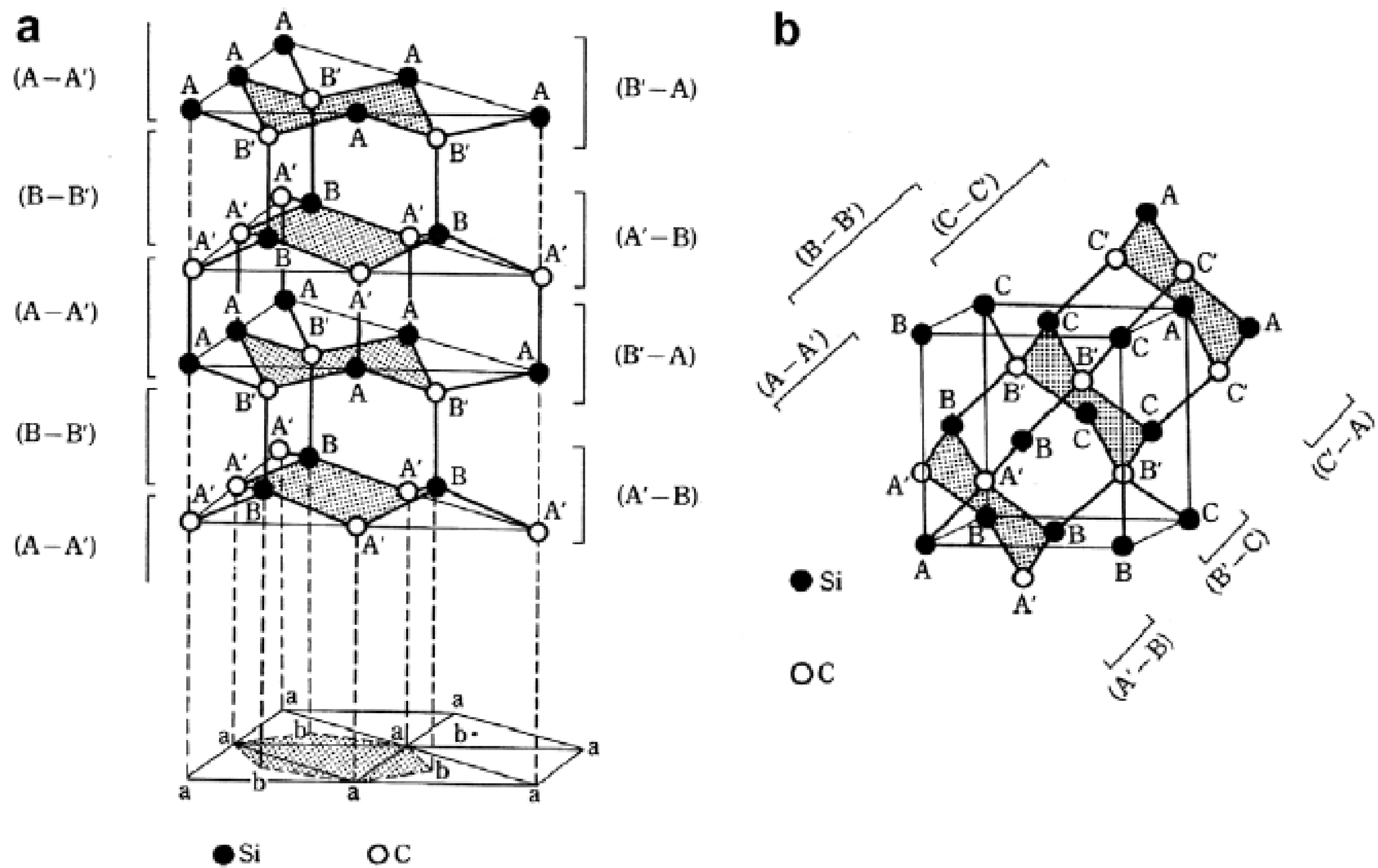

Possibility for using of SiC materials in nuclear energy systems:

- fuel element in high temperature gas-cooled reactor (HTGR)
- fuel blocks for the gas fast reactors (GFR)
- guide tubes materials in very high temperature reactors (VHTR)
- test blanket module designs for the ITER

Schematic illustration of fuel elements: nonirradiated (a) and irradiated (b)

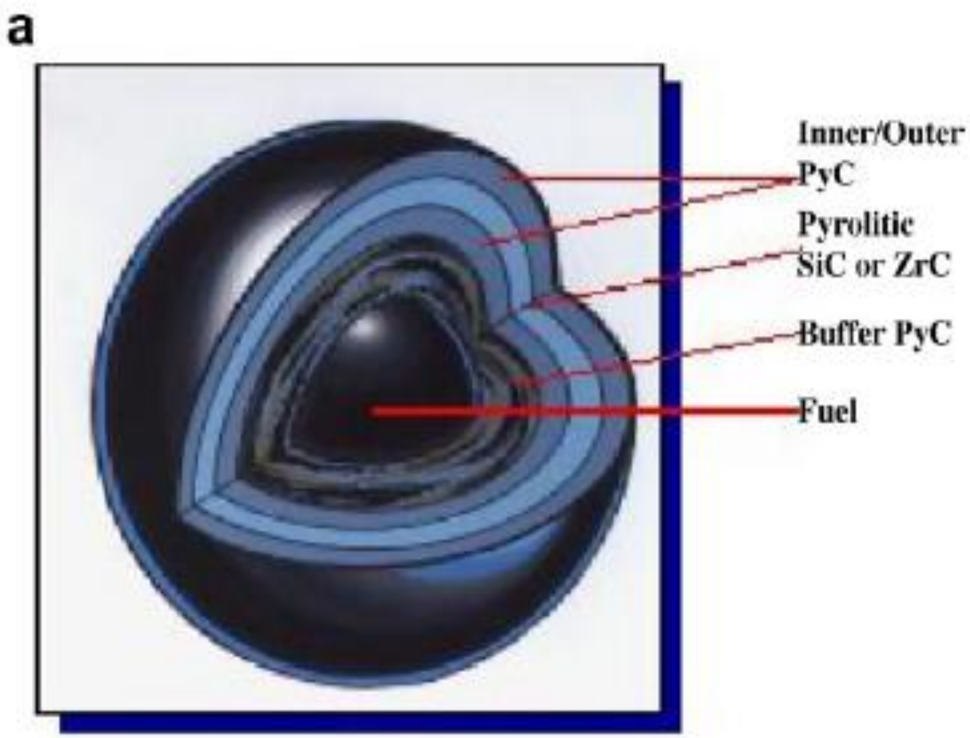

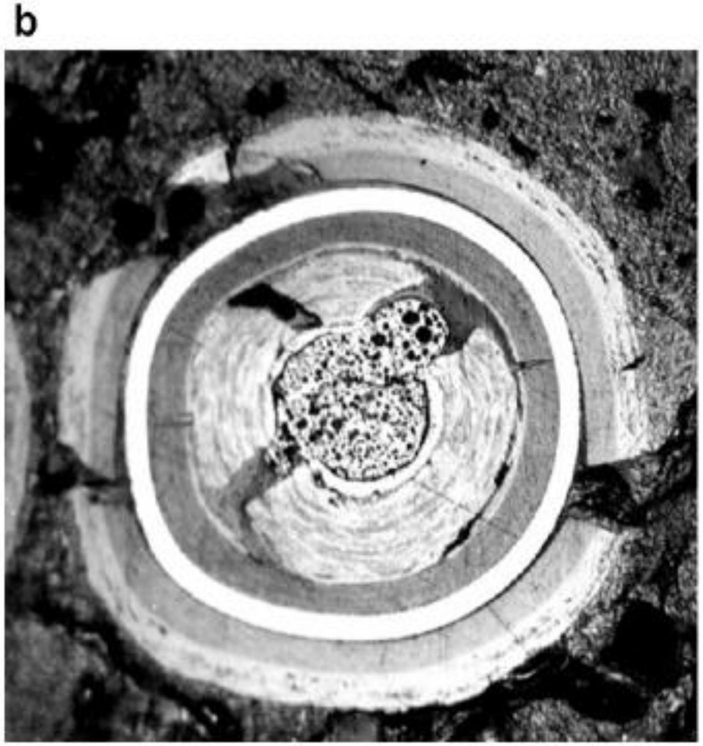

ORNL

Initial microstructure of SiC before fast particle irradiation obtained by TEM on TITAN 80-300 (FEI, US)

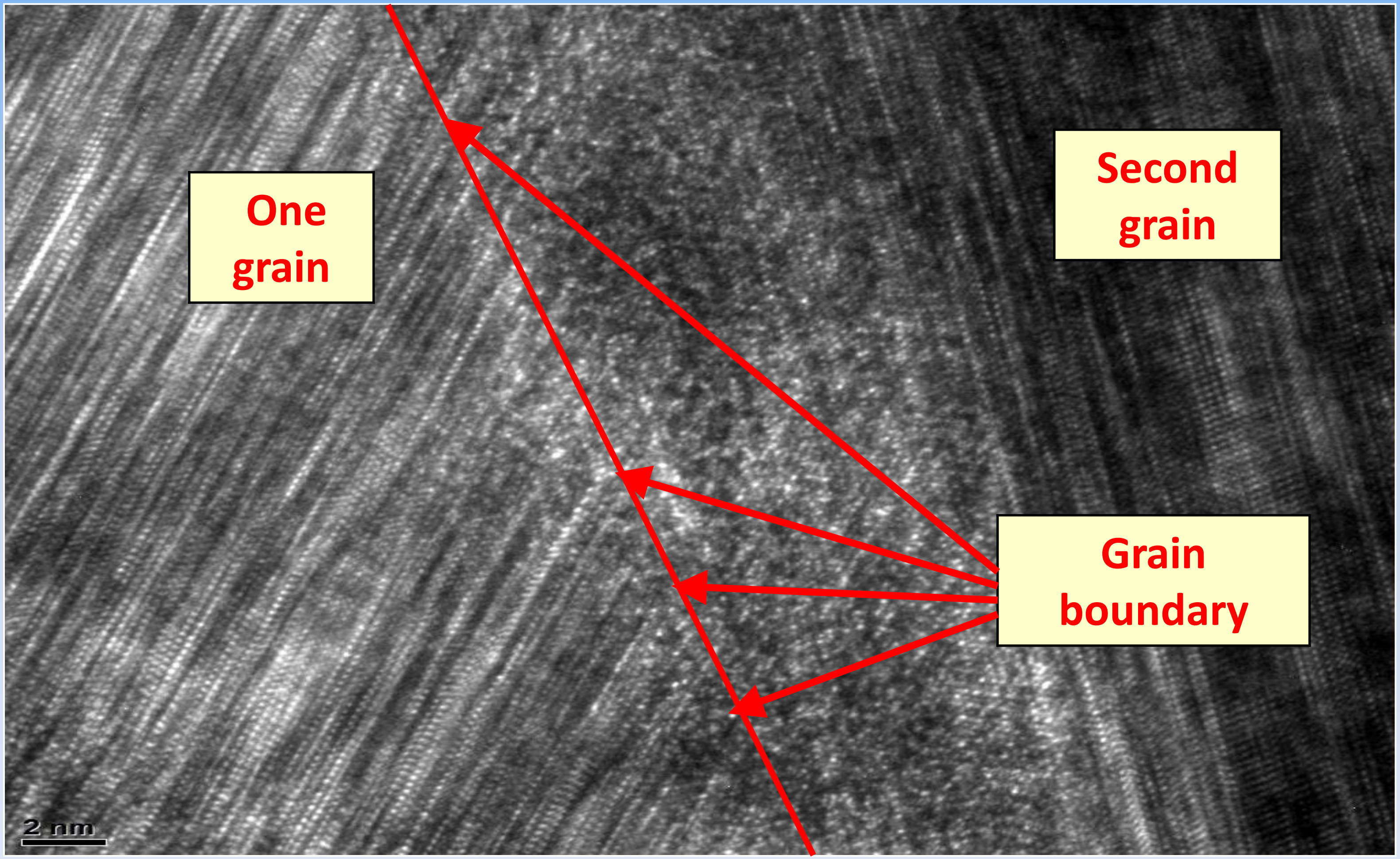

Initial microstructure of SiC before fast particle irradiation obtained by TEM on TITAN 80-300 (FEI, US)

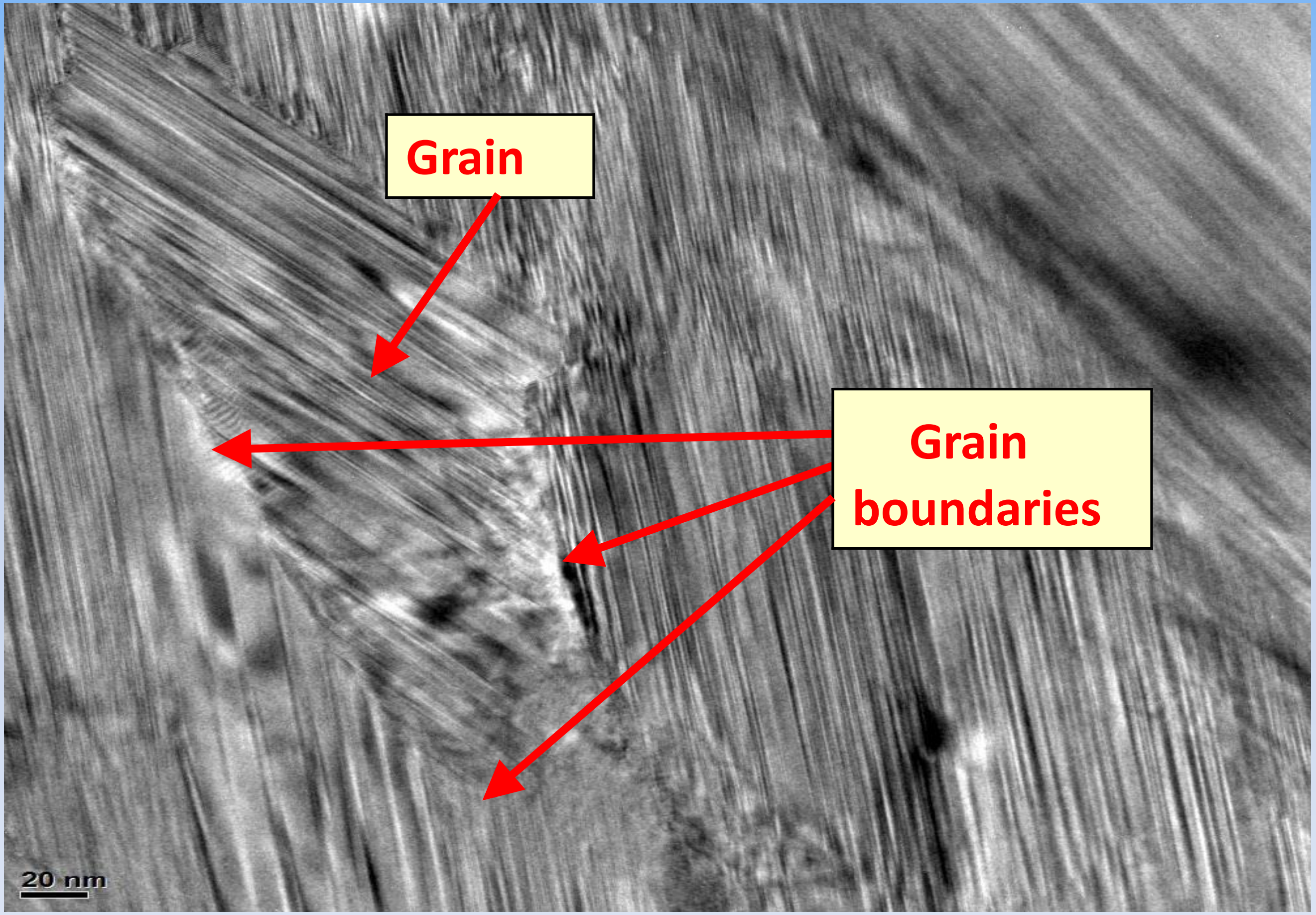

Initial microstructure of SiC before fast particle irradiation obtained by TEM on TITAN 80-300 (FEI, US)

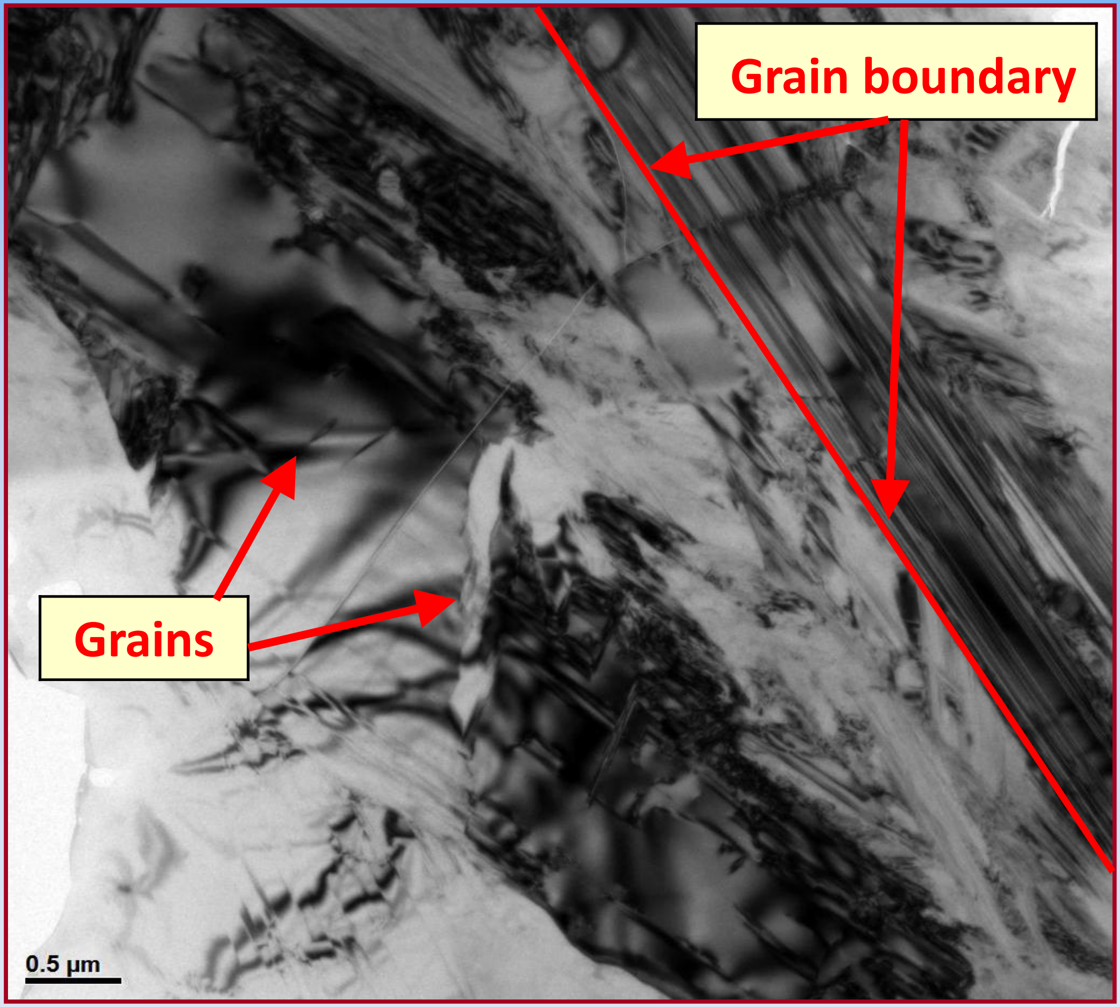

Initial microstructure of SiC before fast particle irradiation obtained by TEM on TITAN 80-300 (FEI, US)

Initial microstructure of SiC before fast particle irradiation obtained by TEM on TITAN 80-300 (FEI, US)

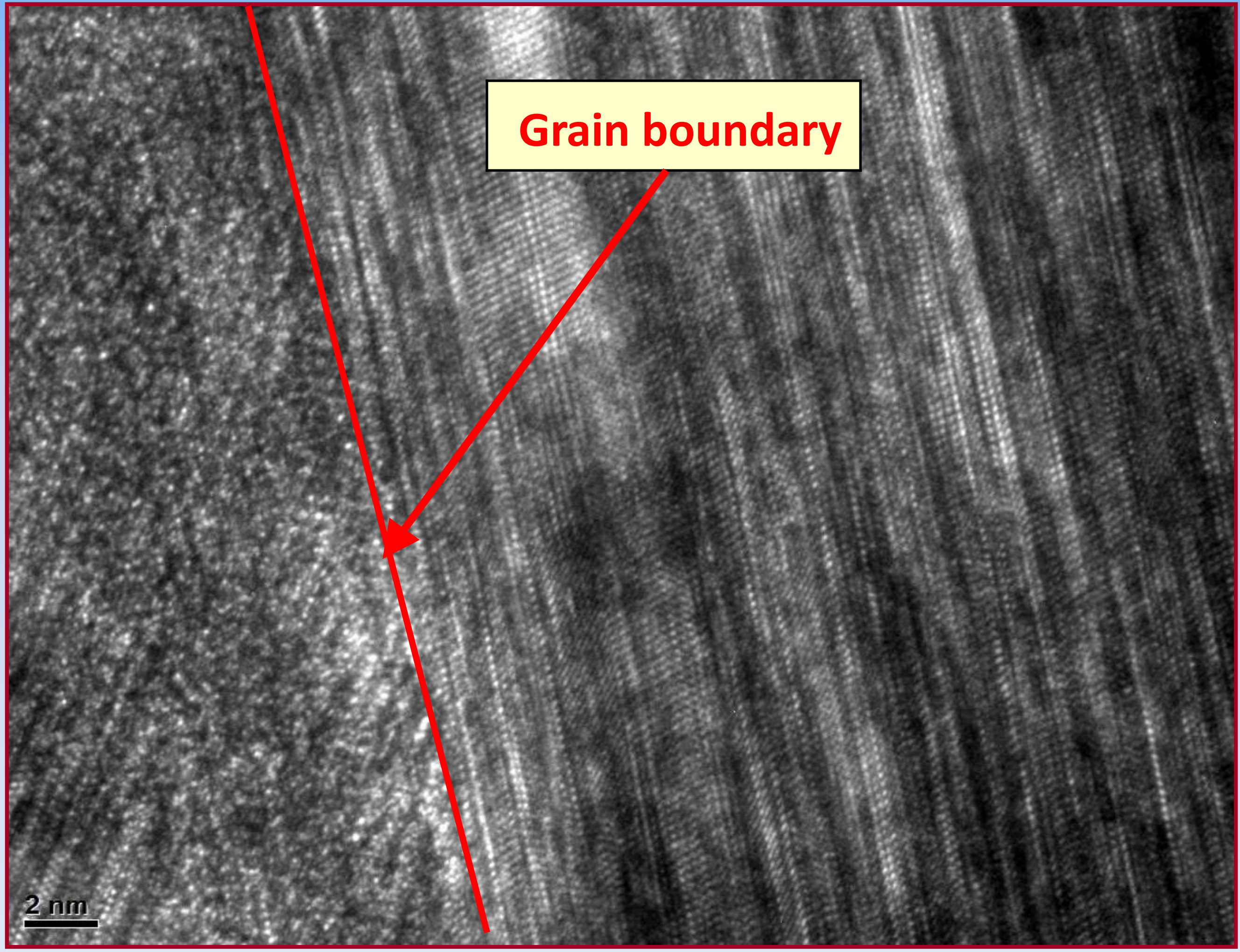

Initial microstructure of SiC before fast particle irradiation obtained by TEM on TITAN 80-300 (FEI, US)

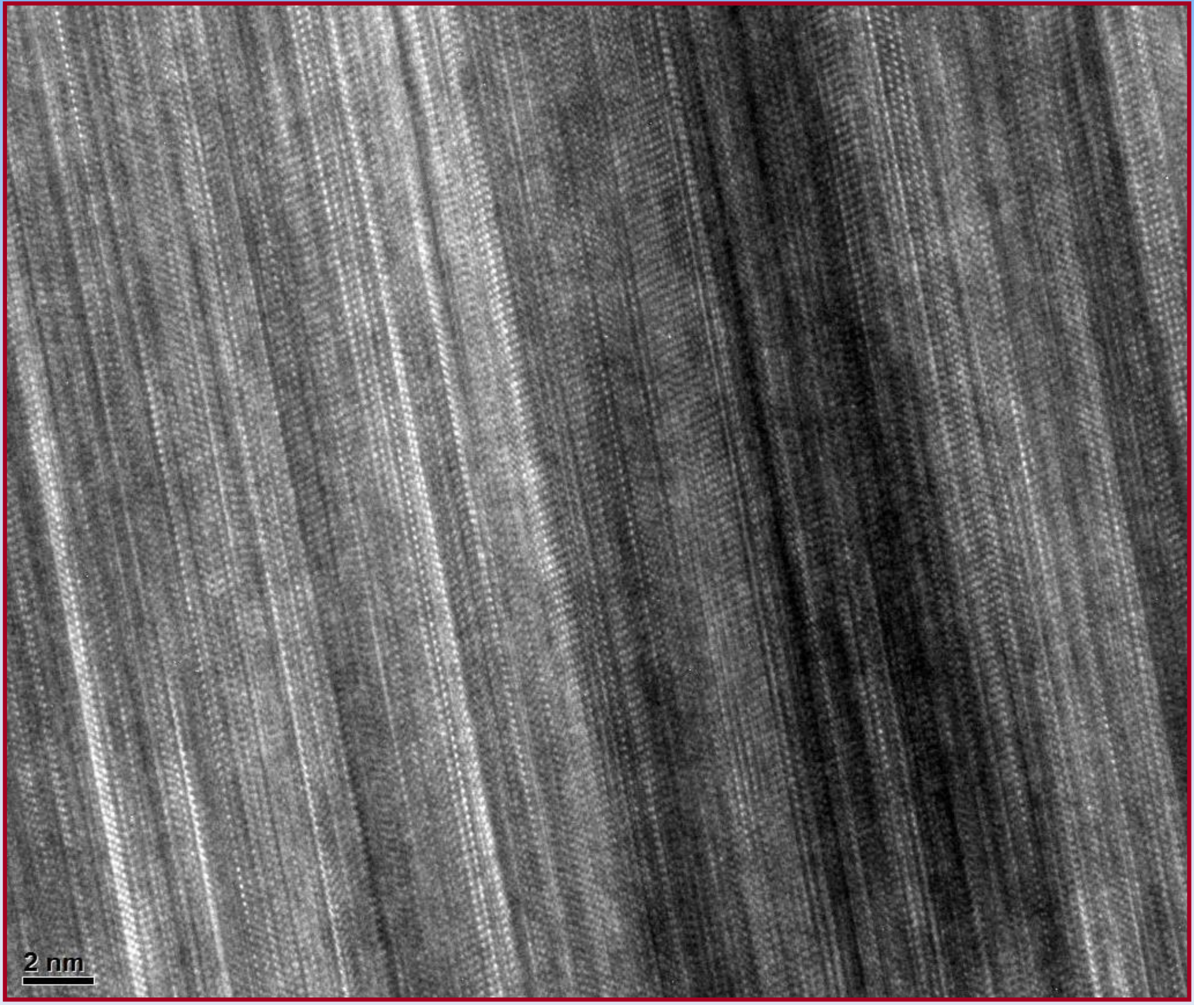

Theoretical Modeling of Radiation Damage Formation in SiC under Fast Proton and Carbon Ion Irradiations

Primary Recoil Spectra for C and Si in Several Neutron Environments

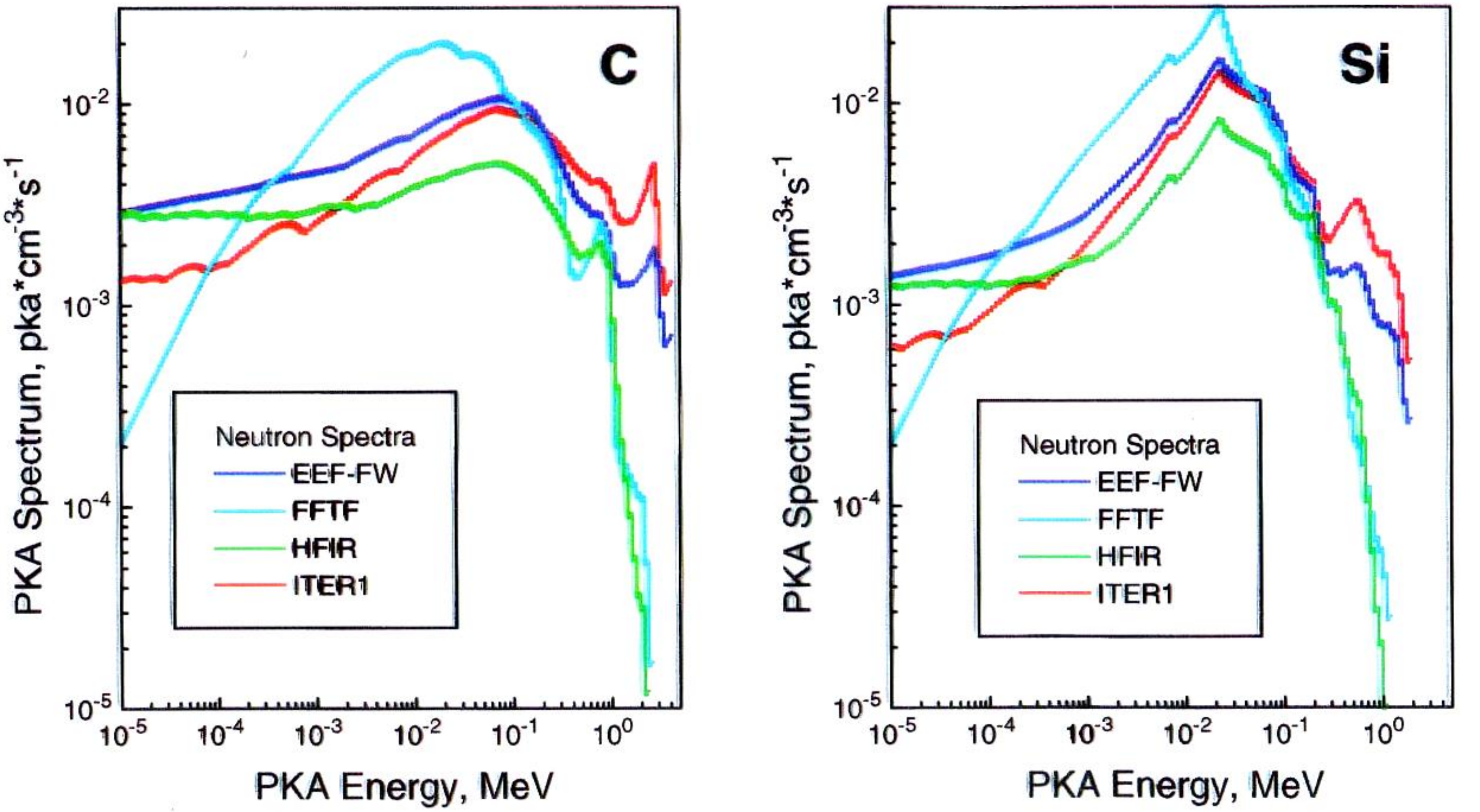

Displacement damage rate in SiC for several neutron and ion sources. All neutron fluxes are normalized to the total flux of 10E18n/m2 s and the light ions to a beam current 10E-2 A/m2

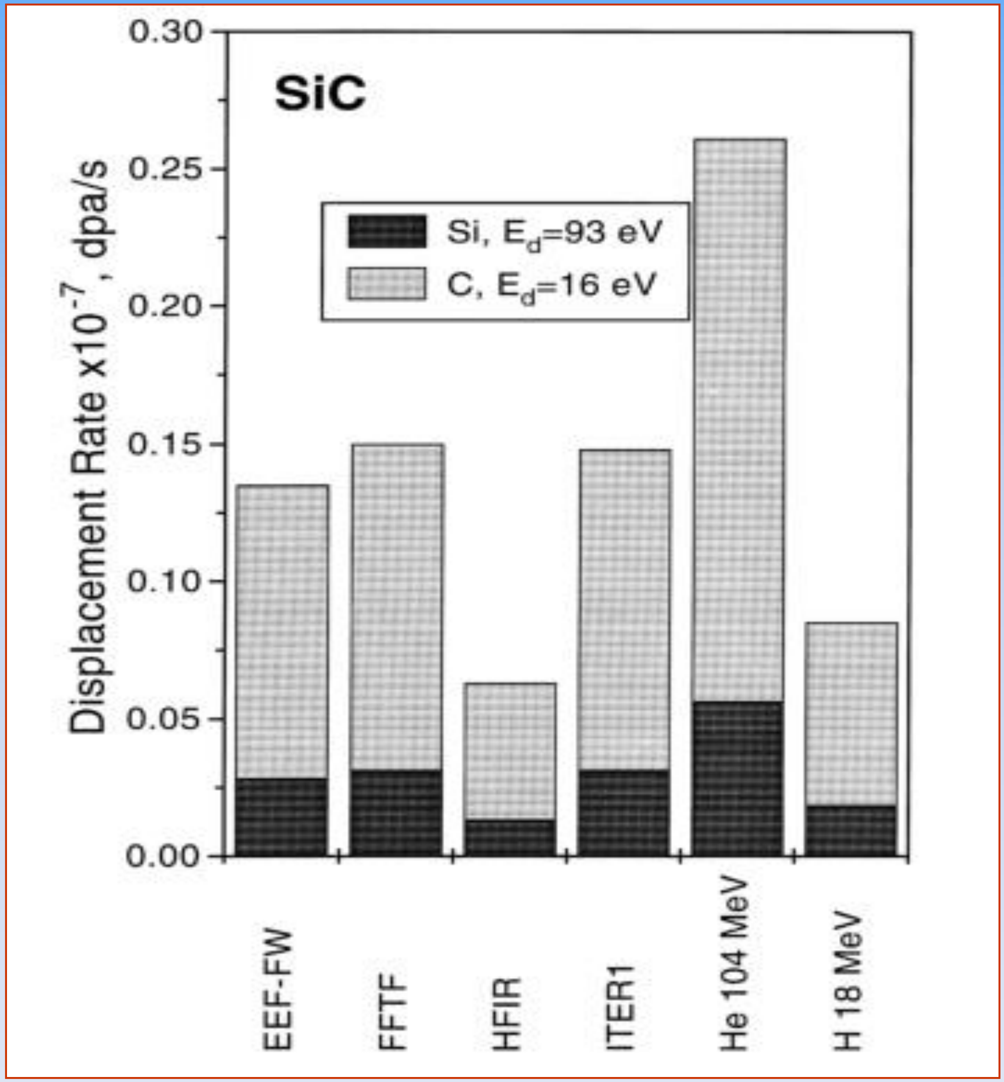

Generation rate of Point defects in SiC under neutron irradiation: HFIR and ITER.

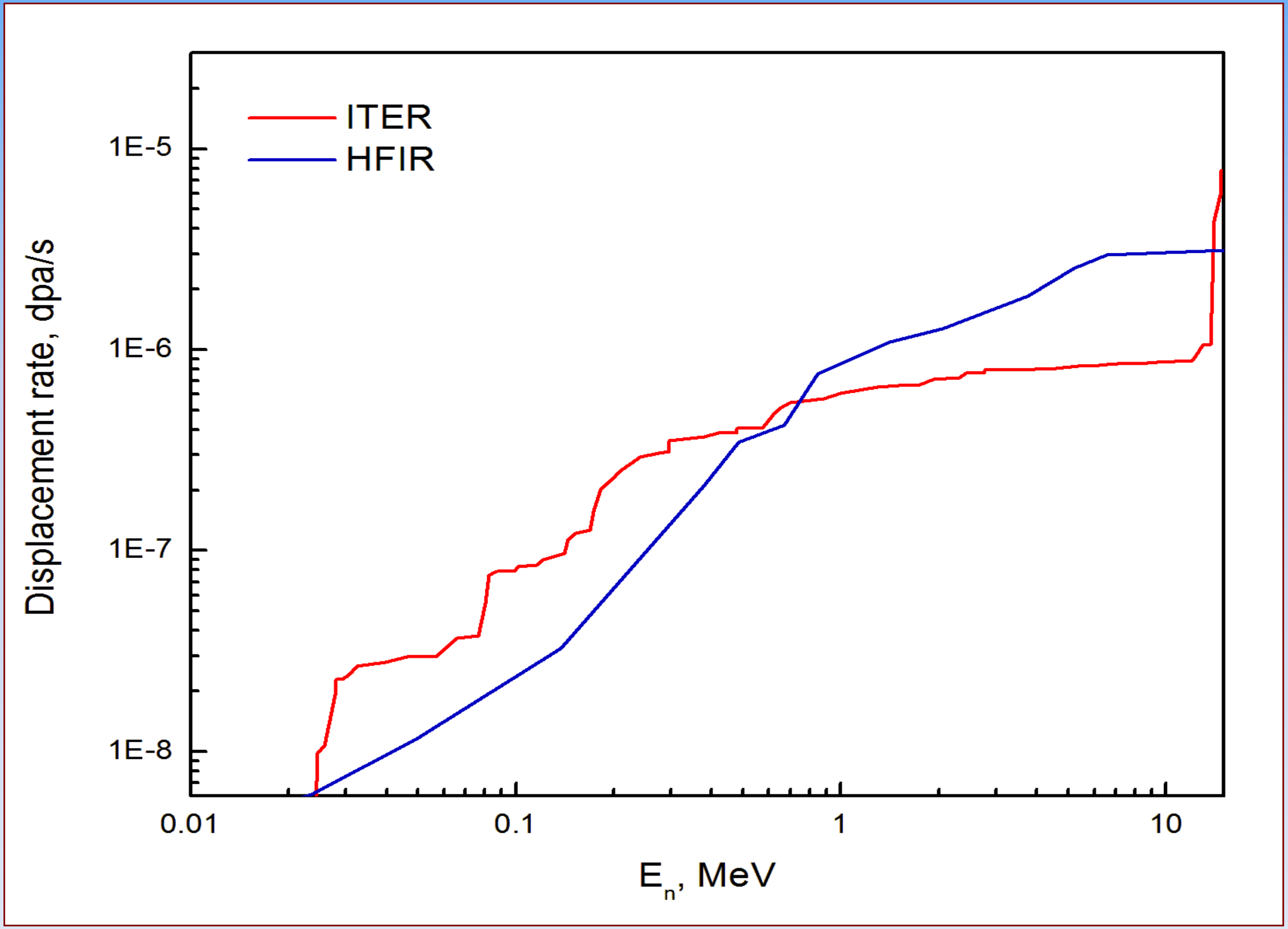

Displacement cross sections for secondary pions with energies up to 450 GeV in graphite and copper

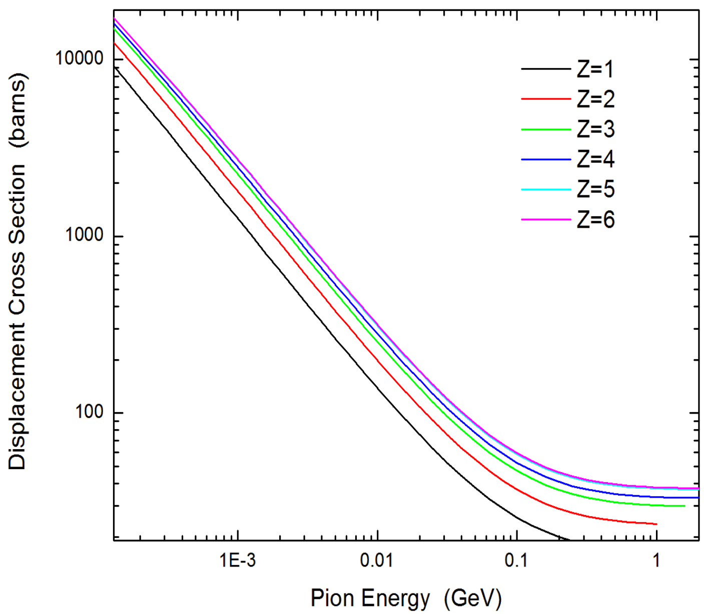

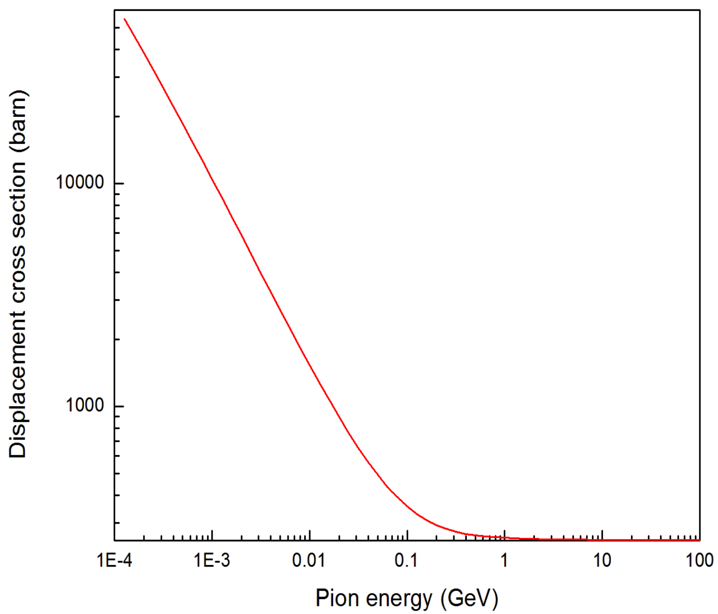

Graphite

Copper

Displacement cross sections for secondary electrons with energies up to 450 GeV in graphite and copper

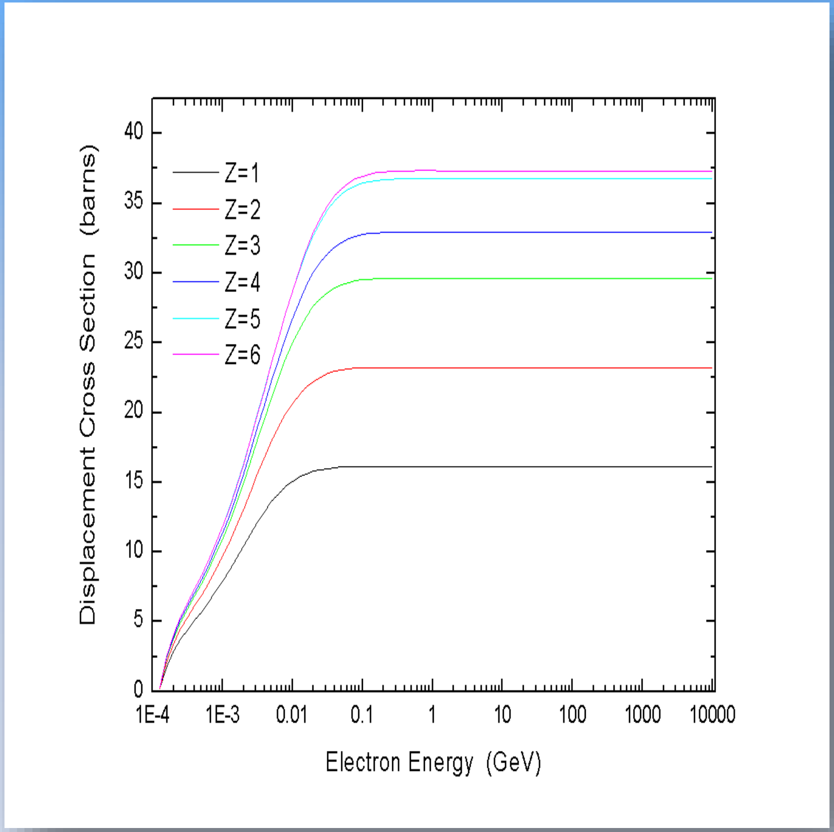

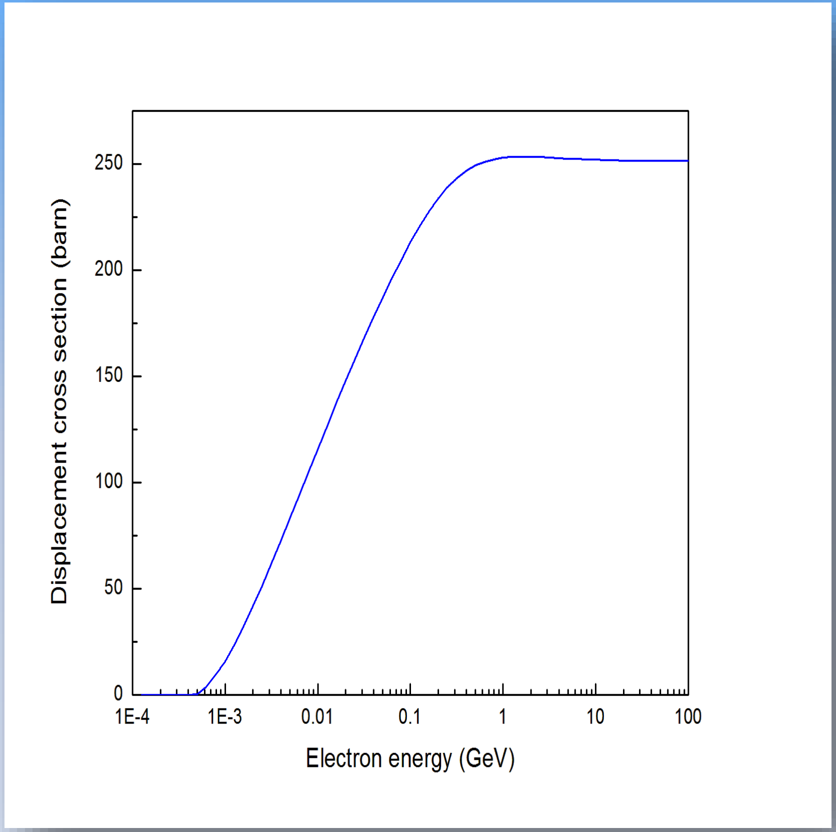

Graphite

Copper

The spectrum of pions (π^-) produced in graphite at different distances along the beam of 450 GeV protons (FLUKA)

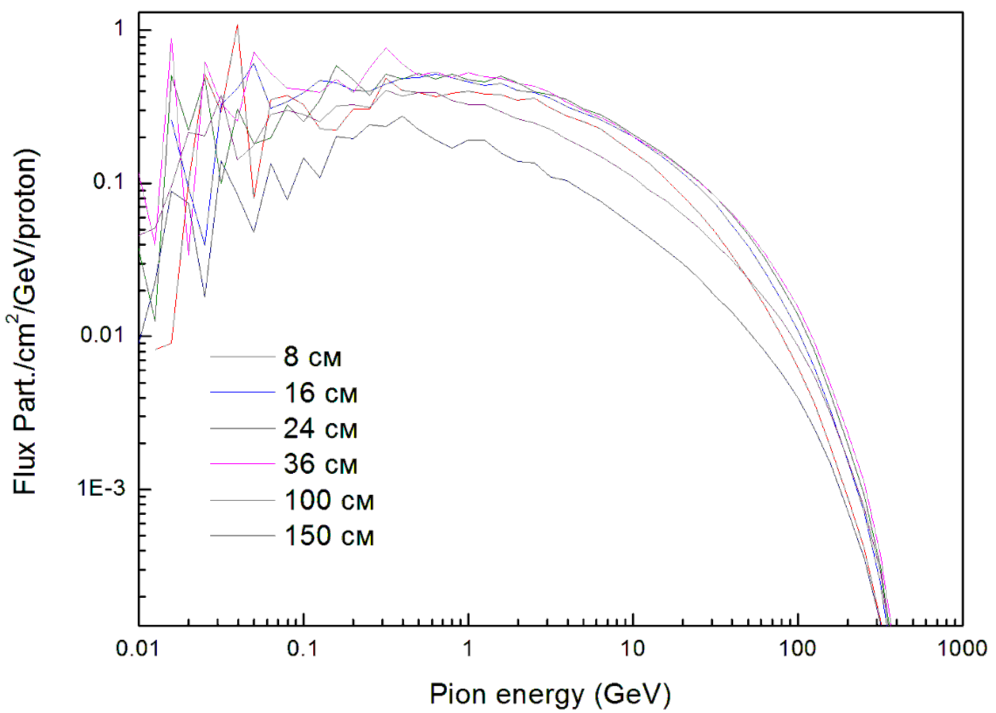

The spectrum of secondary relativistic electrons produced in graphite at different distances along the beam with energy 450 GeV protons (FLUKA)

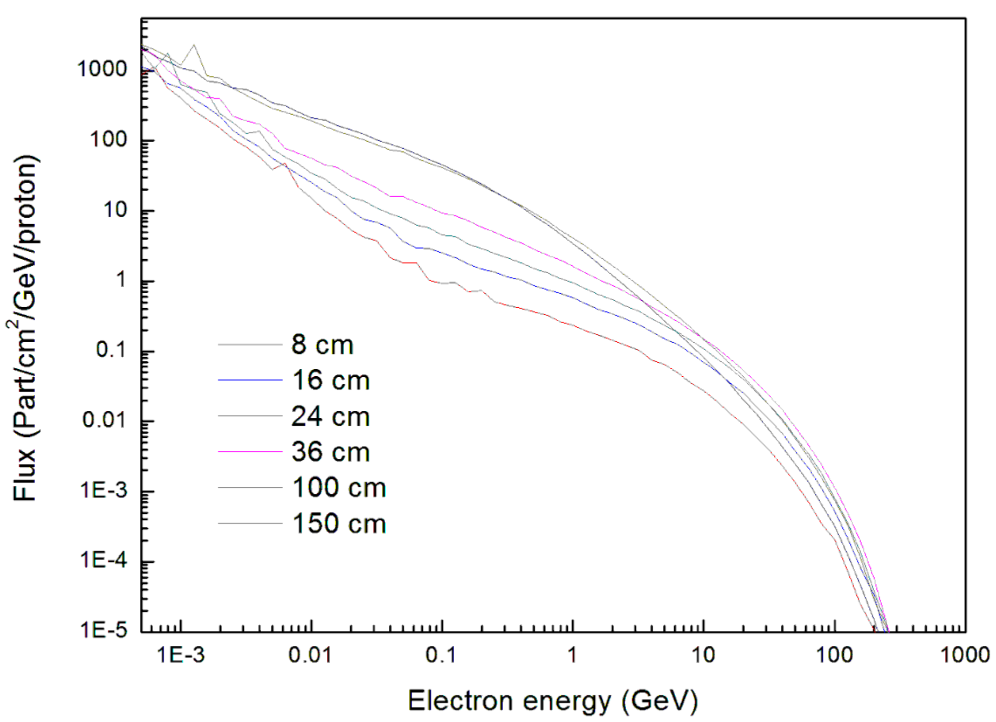

The spectrum of pions produced in graphite at different distances along the beam of 7 TeV protons (FLUKA)

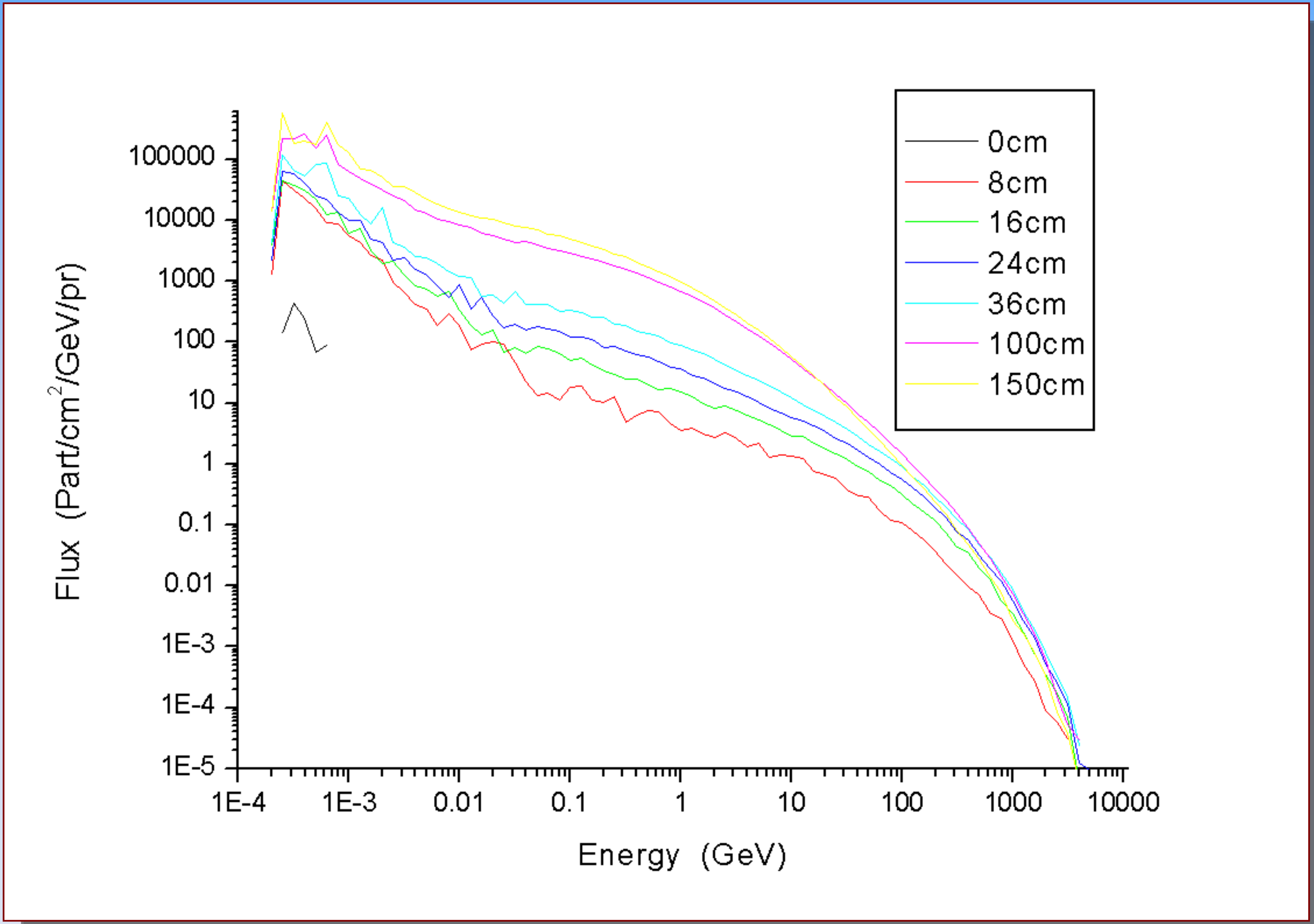

Generation rate of primary radiation point defects in graphite versus energy of pions for a single bunch of 450 GeV protons

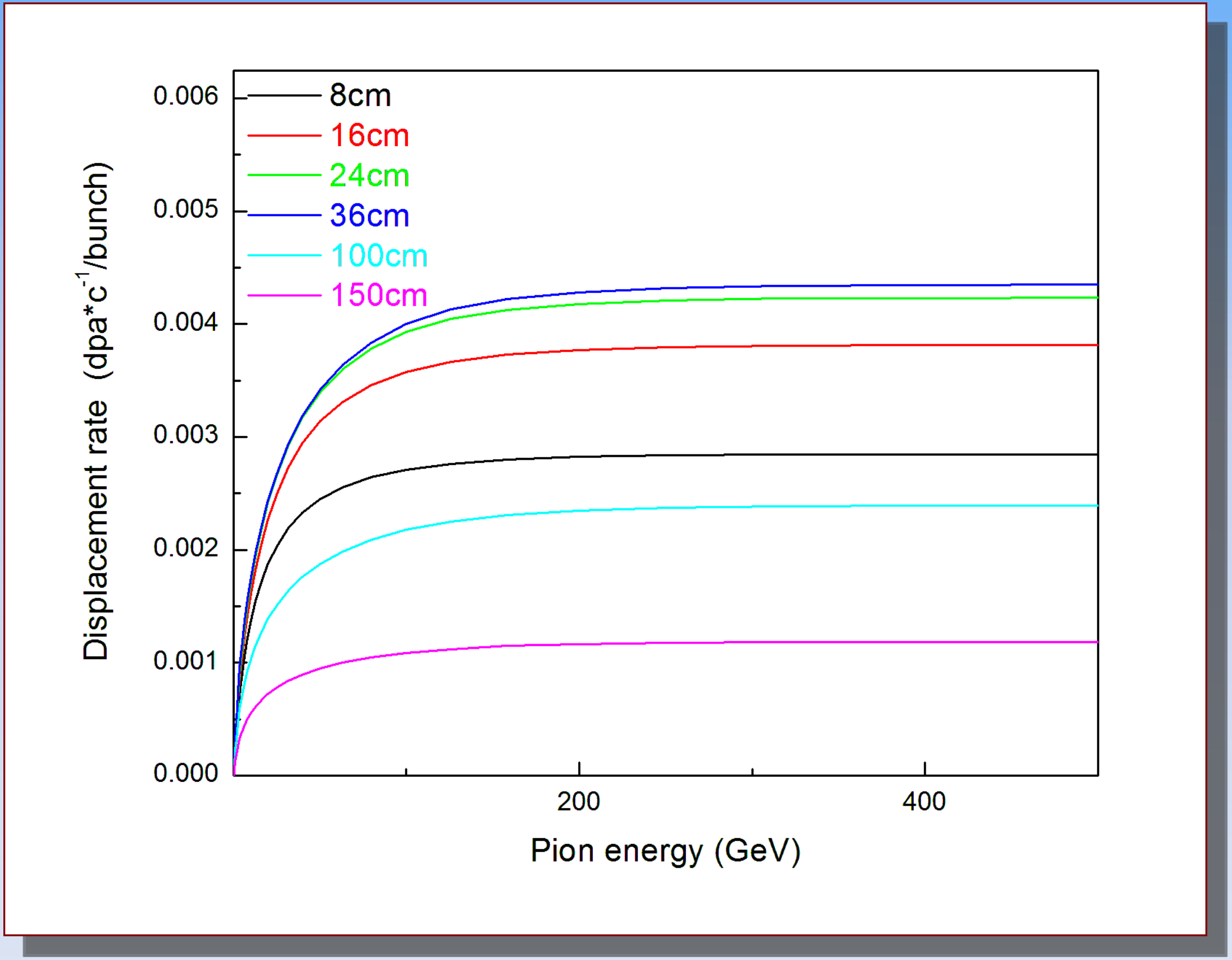

Generation rate of primary radiation point defects in graphite versus energy of secondary electrons for a single bunch of 450 GeV protons

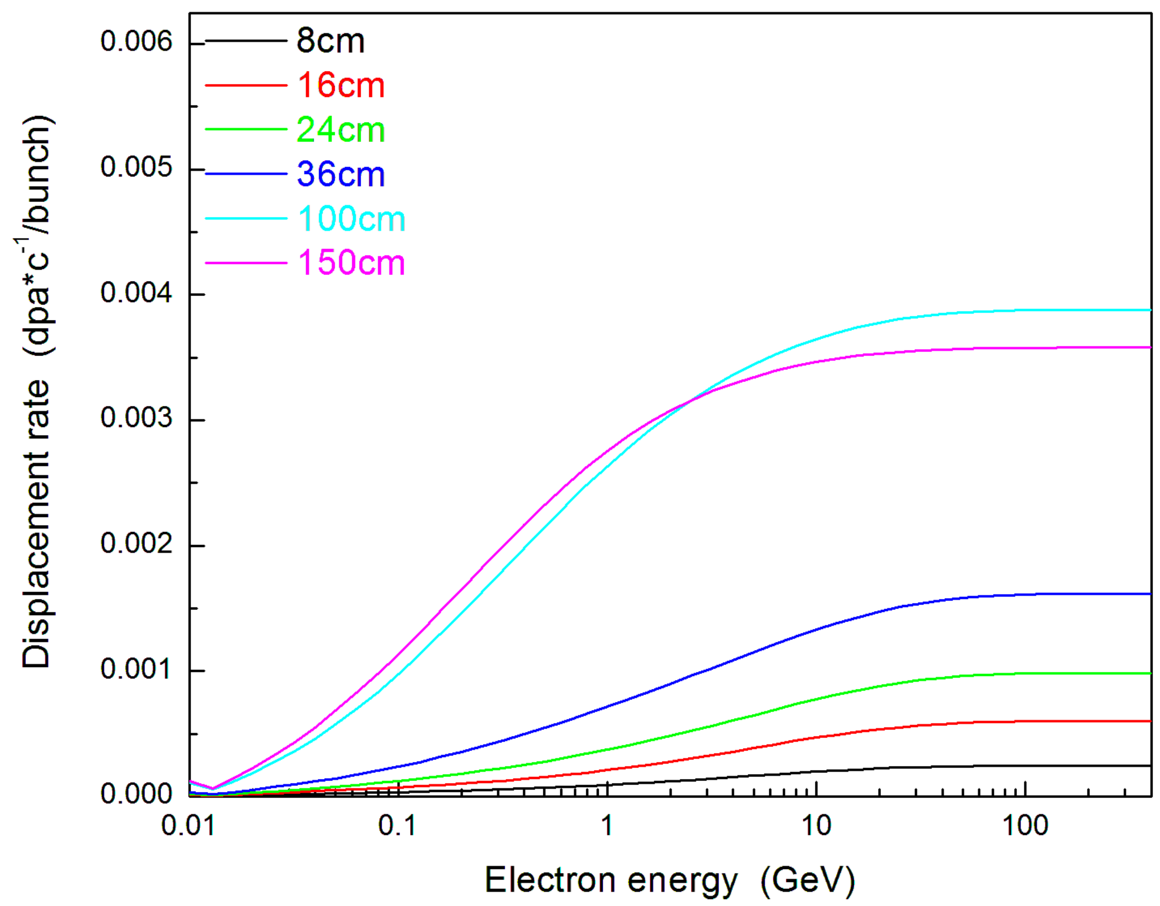

Displacement rate of point defects (DPA) per each bunch produced by different secondary particles at different distances in graphite along the 7 TeV proton LHC beam

protons

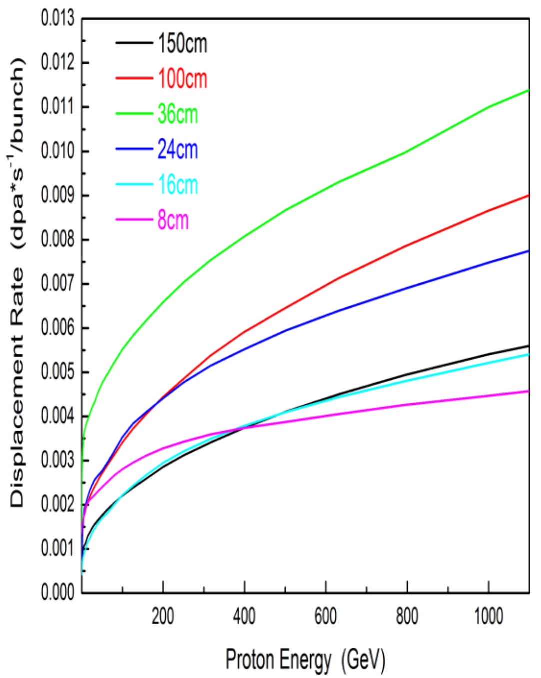

Max DPA/s – 0.012 dpa/s

pions

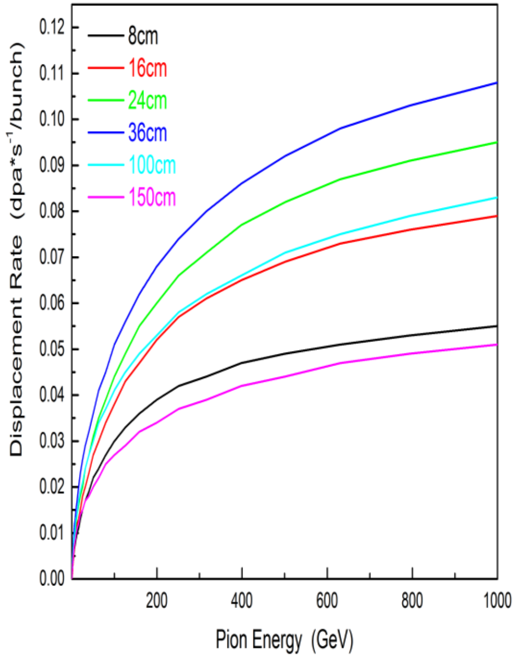

Max DPA/s – 0.11 dpa/s

neutrons

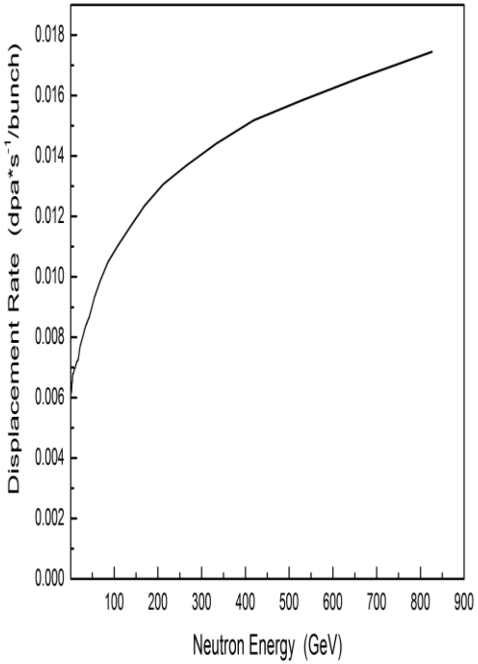

Max DPA/s – 0.018 dpa/s

Displacement rate of point defects (DPA) per each bunch produced by different secondary particles at different distances in graphite along the 450 GeV proton LHC beam

pions

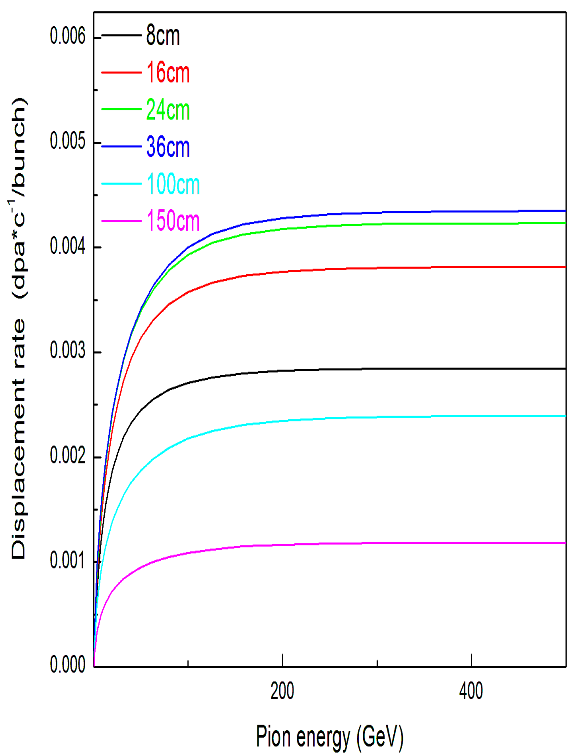

Max DPA/s – 0.0043 dpa/s

electrons

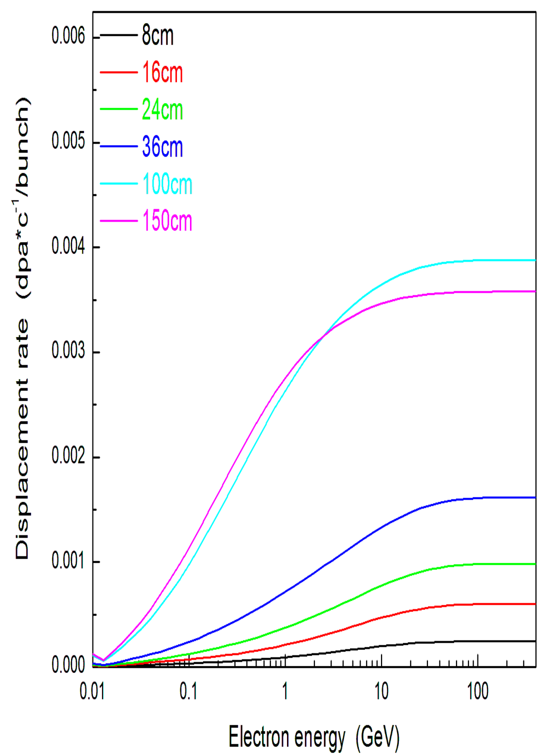

Max DPA/s – 0,004 dpa/s

neutrons

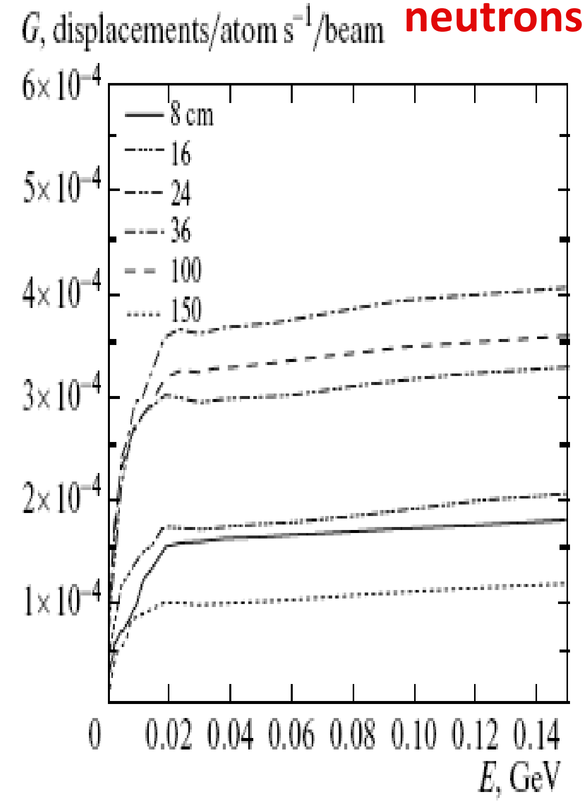

Max DPA/s – 0.0004 dpa/s

Theoretical Modeling of Radiation Damage Formation in SiC under Fast Proton Irradiations on NRC KI cyclotron

Calculations of DPA level in SiC for the protons with the energy 10 MeV and fluence 10E18 p/cm2

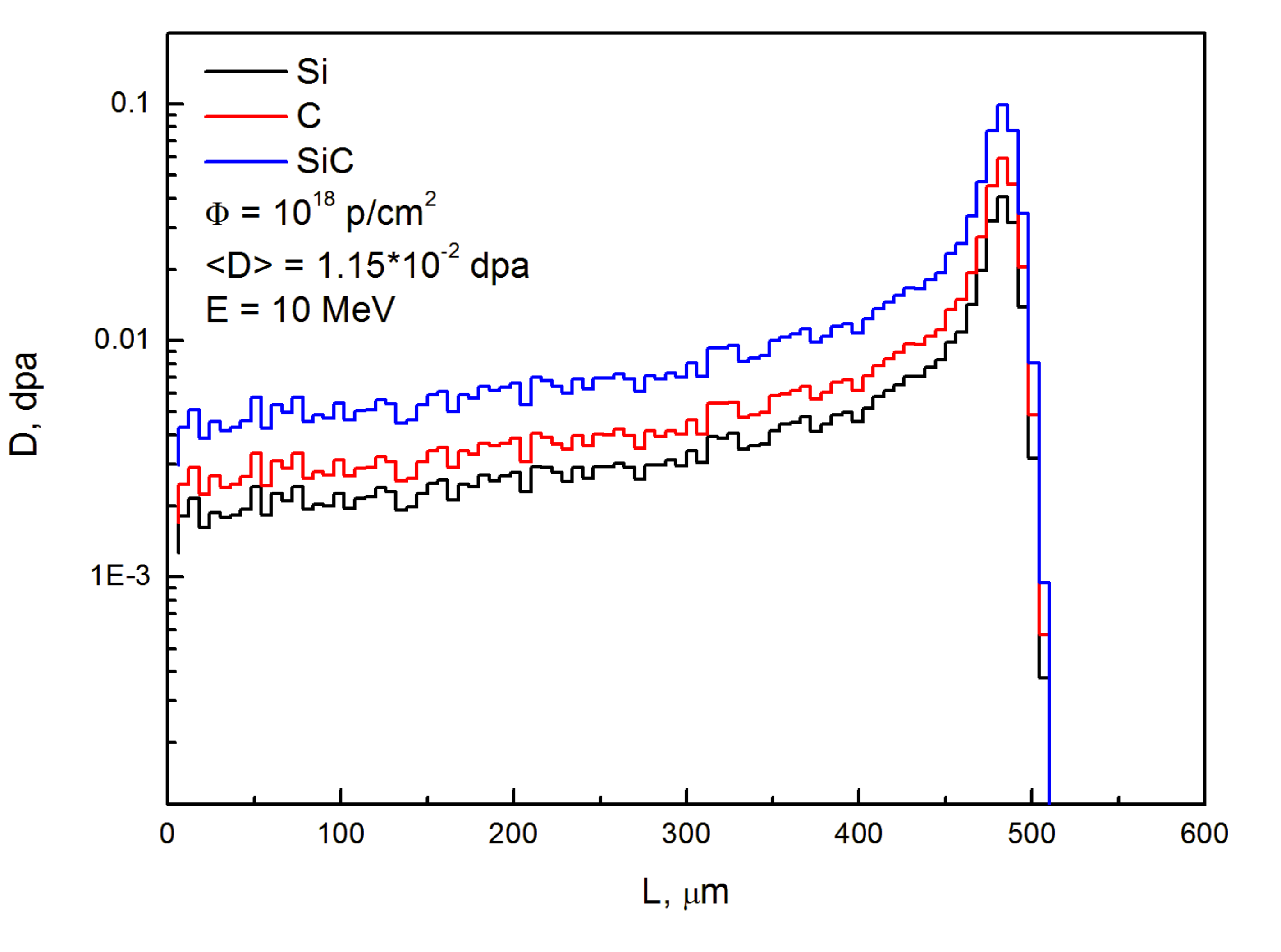

Calculations of DPA level in SiC for protons with the energy 20 MeV and fluence 10E18 p/cm2

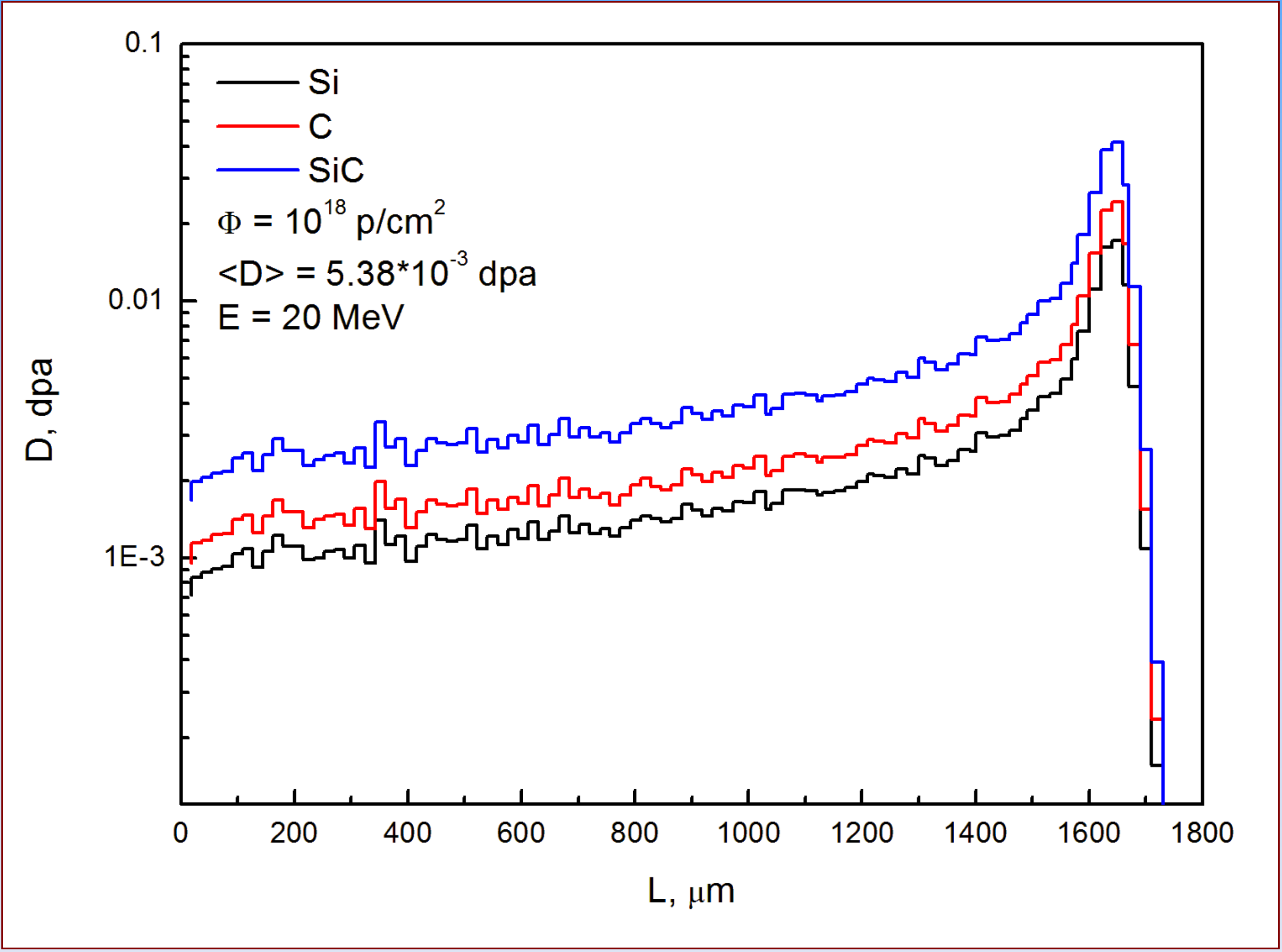

Calculations of DPA level in SiC for the protons with the energy 30 MeV and fluence 10E18 p/cm2

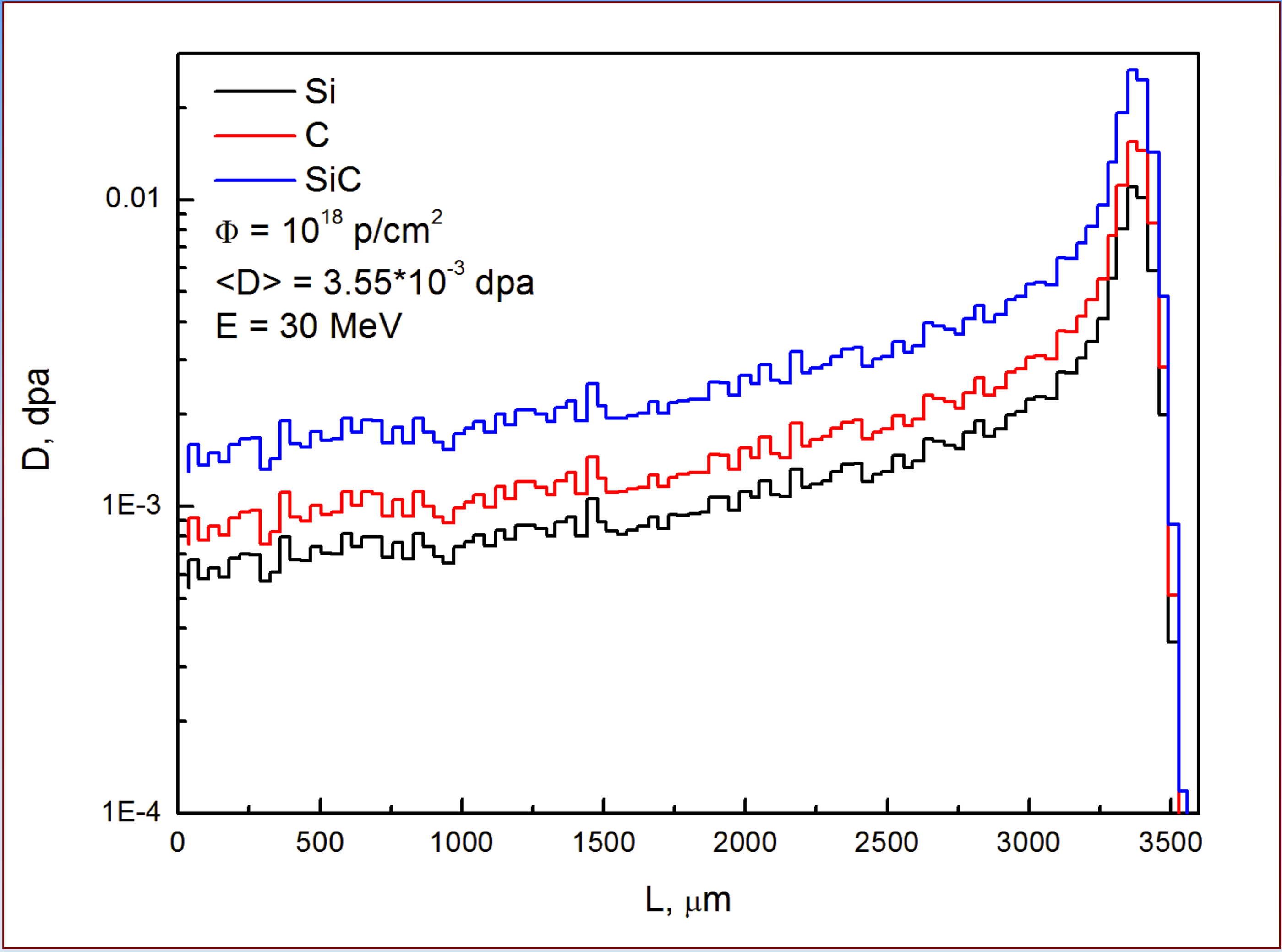

Theoretical Modeling of Radiation Damage Formation in SiC under Fast Carbon Ion Irradiations on NRC KI cyclotron

Calculations of DPA level in SiC for carbon ion irradiation with the energy 10 MeV and fluence 10E17 p/cm2

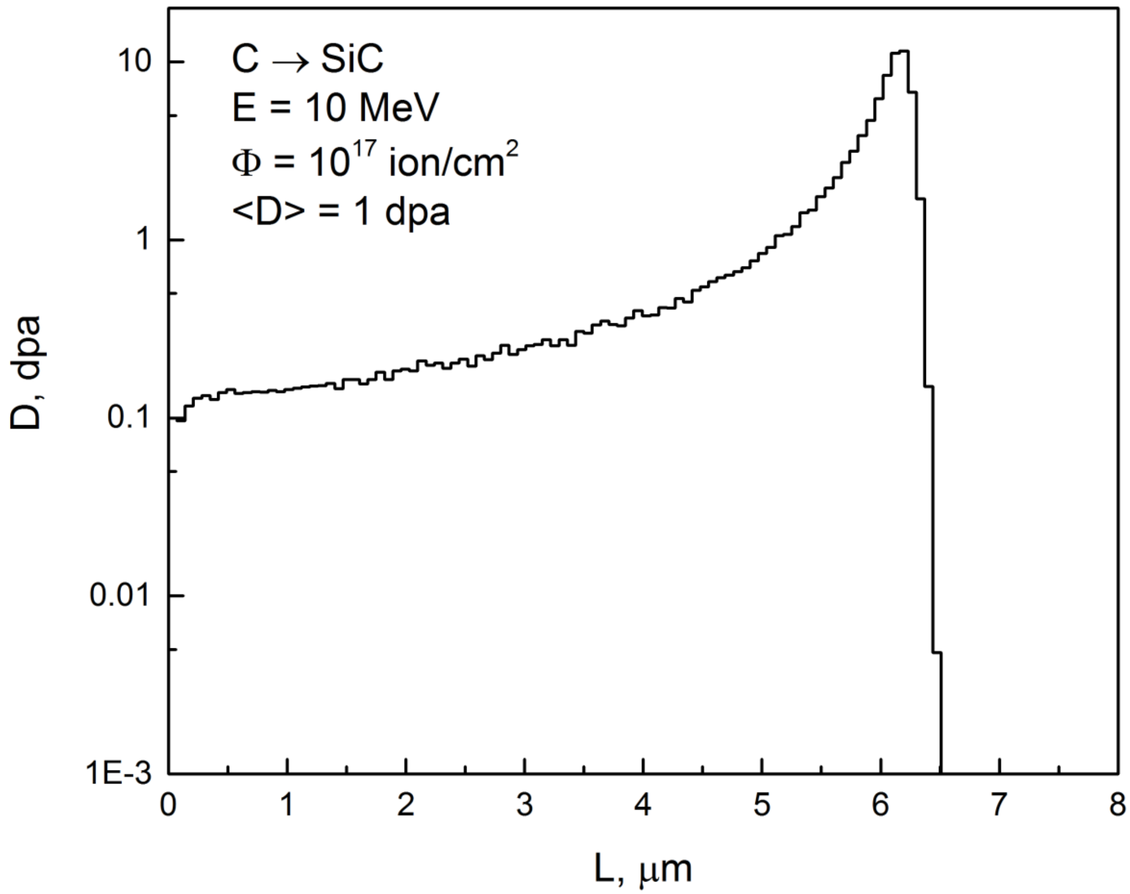

Calculations of DPA level in SiC for carbon ion irradiation with the energy 20 MeV and fluence 10E17 p/cm2

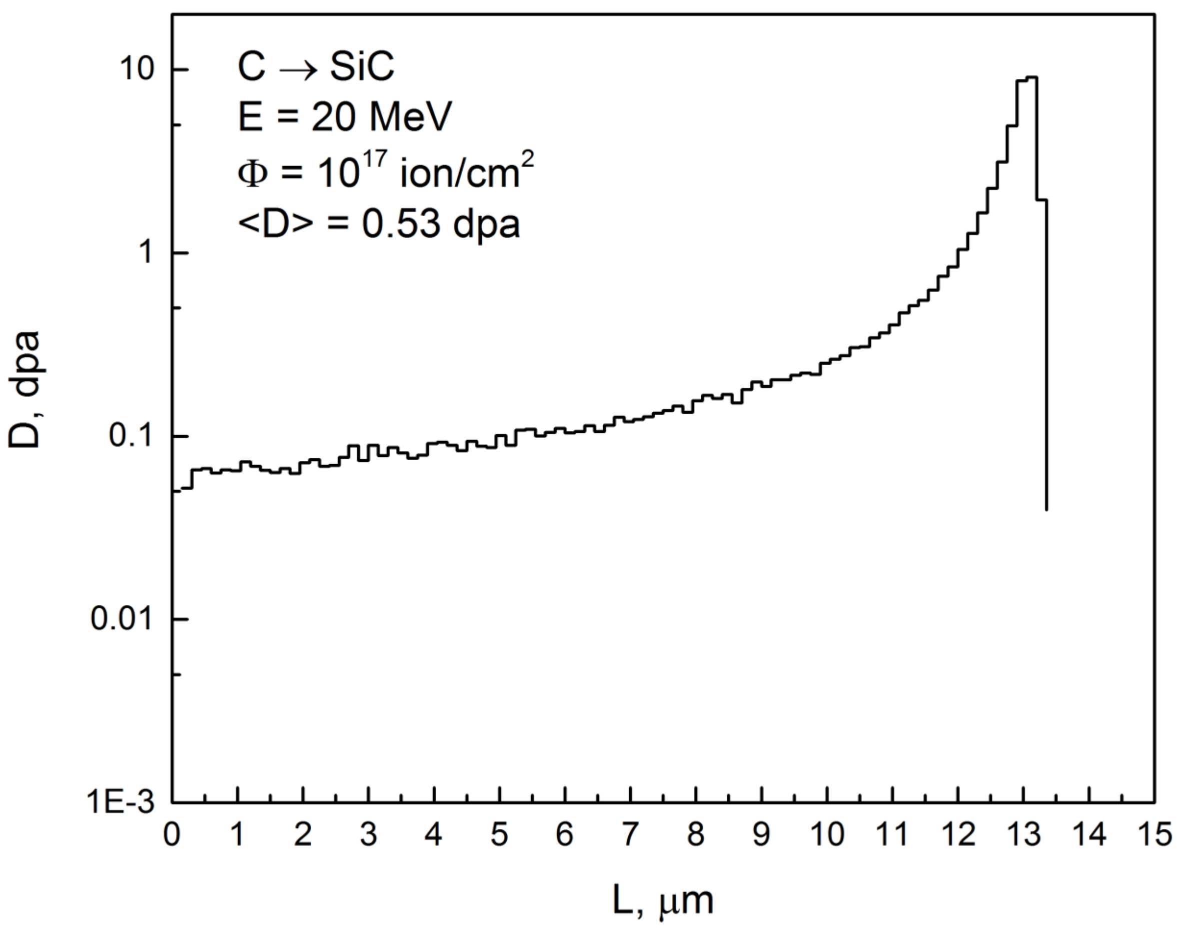

Calculations of DPA level in SiC for carbon ion irradiation with the energy 30 MeV and fluence 10E17 p/cm2

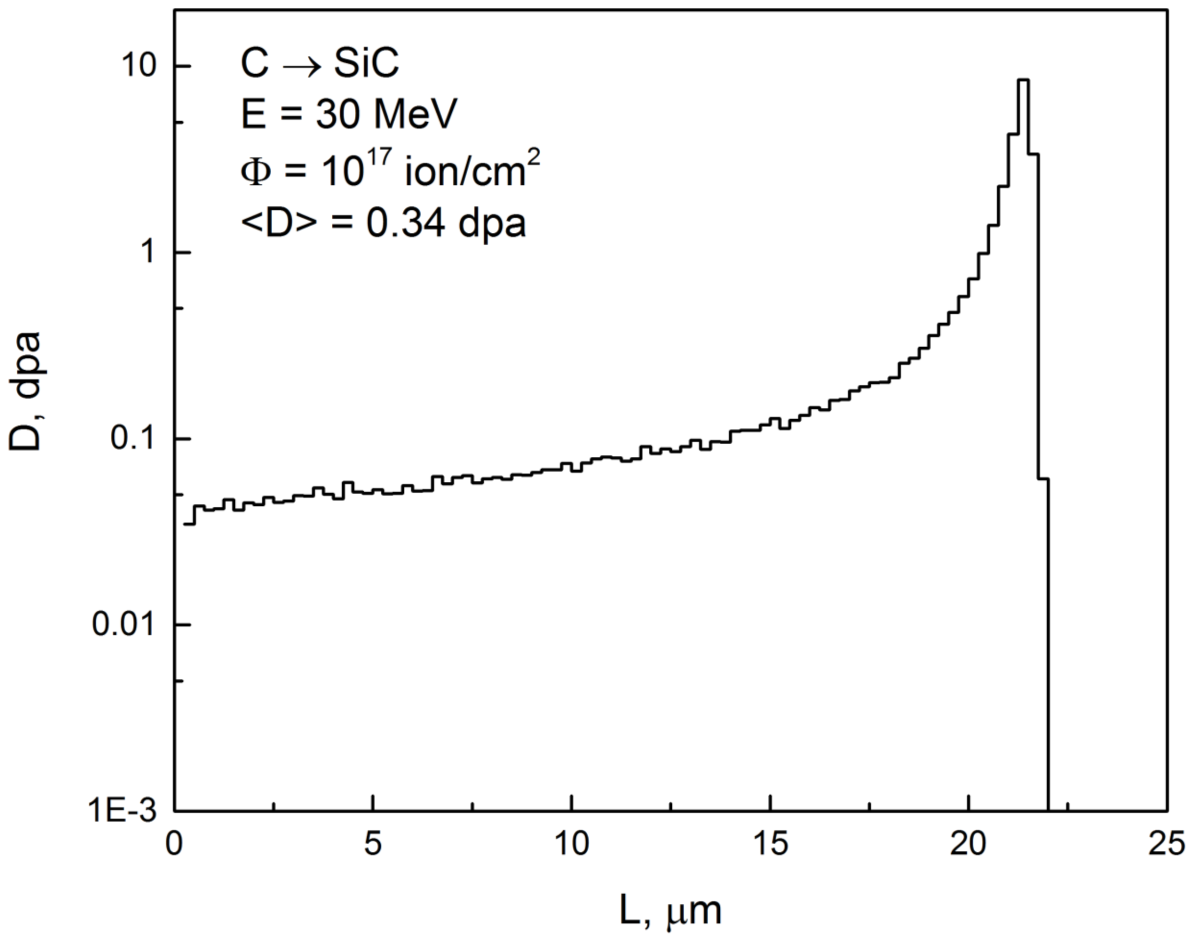

Theoretical Modeling of Cascades and Sub-cascade Formation in SiC under Fast Particle Irradiations

Comparison of cascade and sub-cascade formation in light and heavy materials

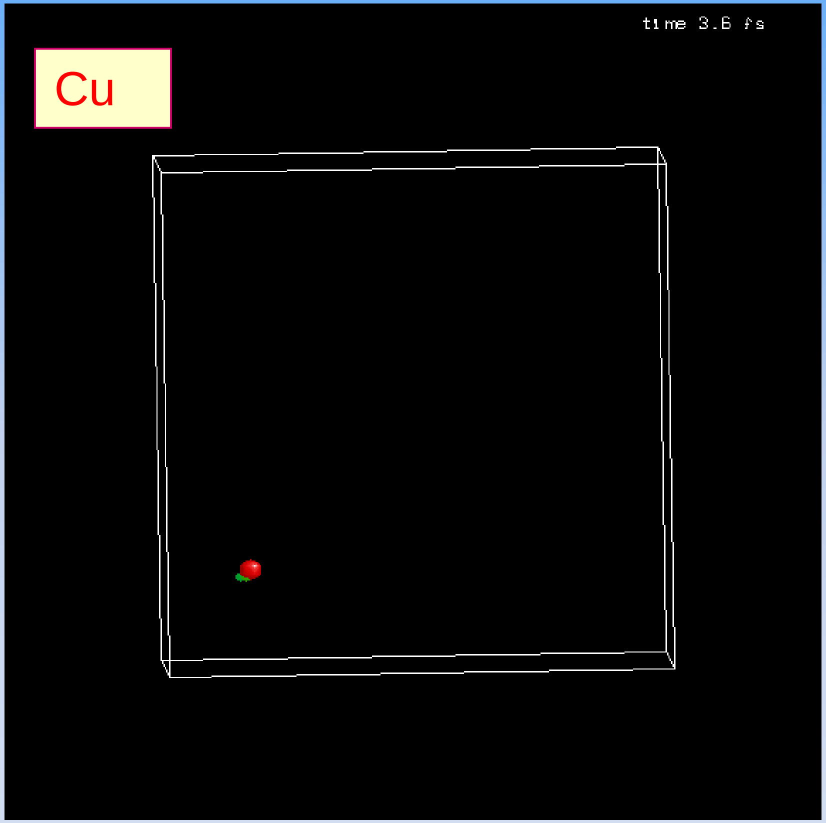

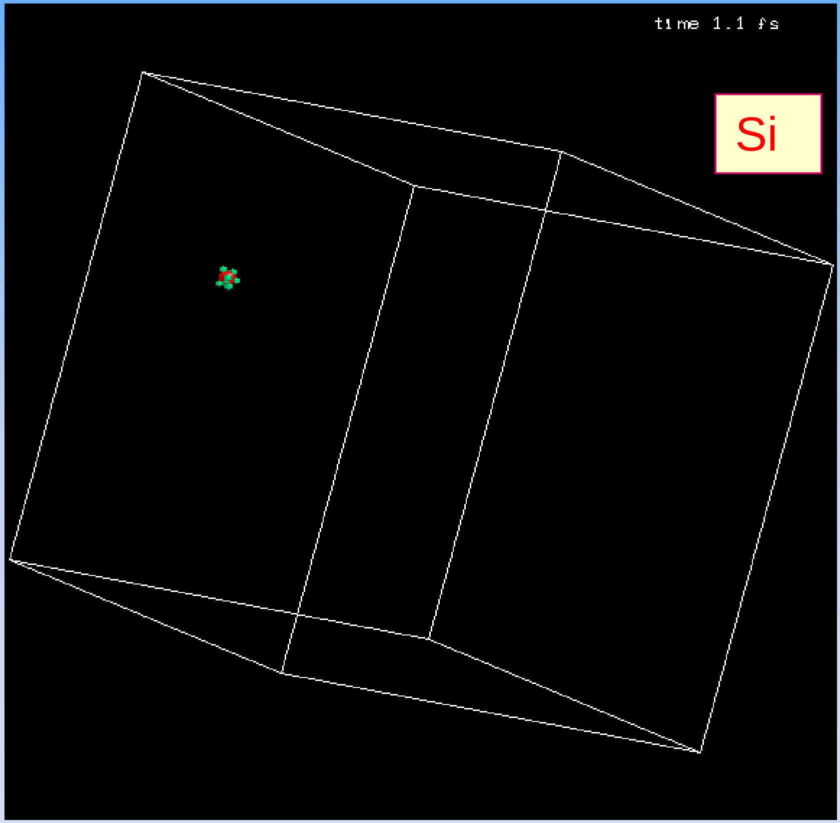

K. Nordlund (1998)

PKA

SKA

λ_{PKA} Mean free path

R_{sub} Average size of damage region

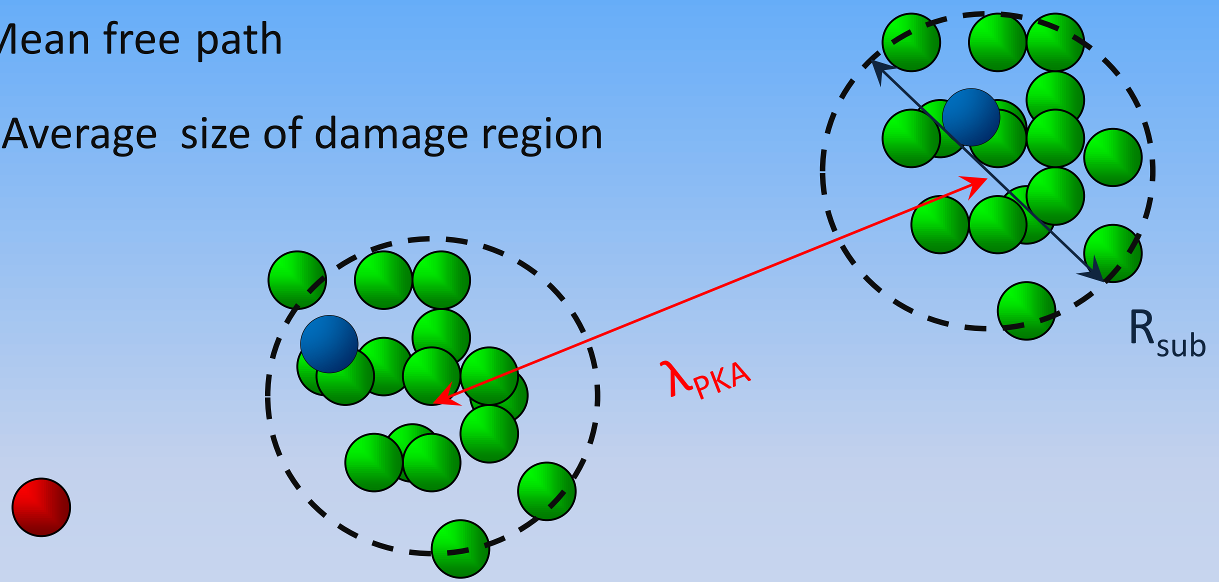

Sub-cascade formation criterion:

$$\lambda_{PKA} \geq R_{sub}$$

Sub-cascade generation rate in graphite and copper versus energy of secondary pions

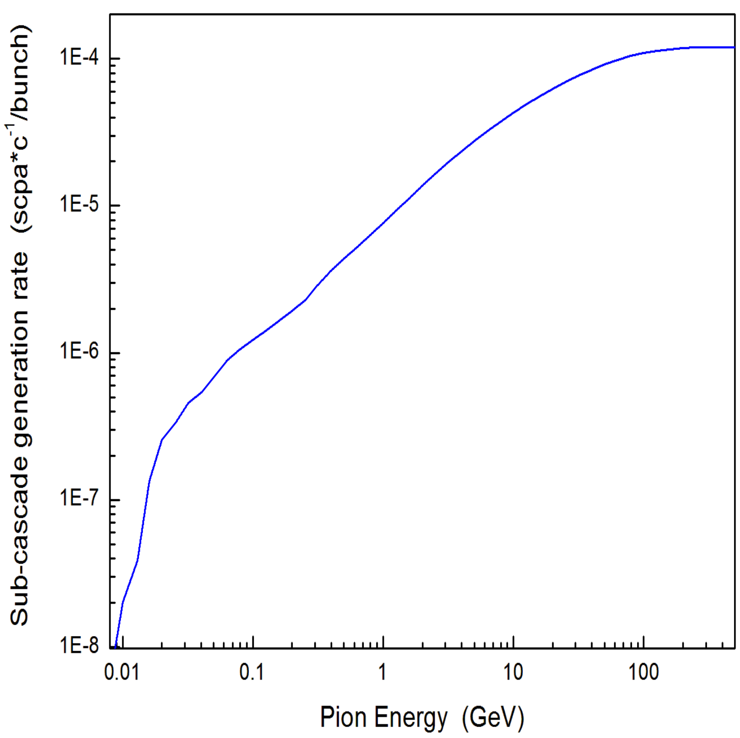

Graphite

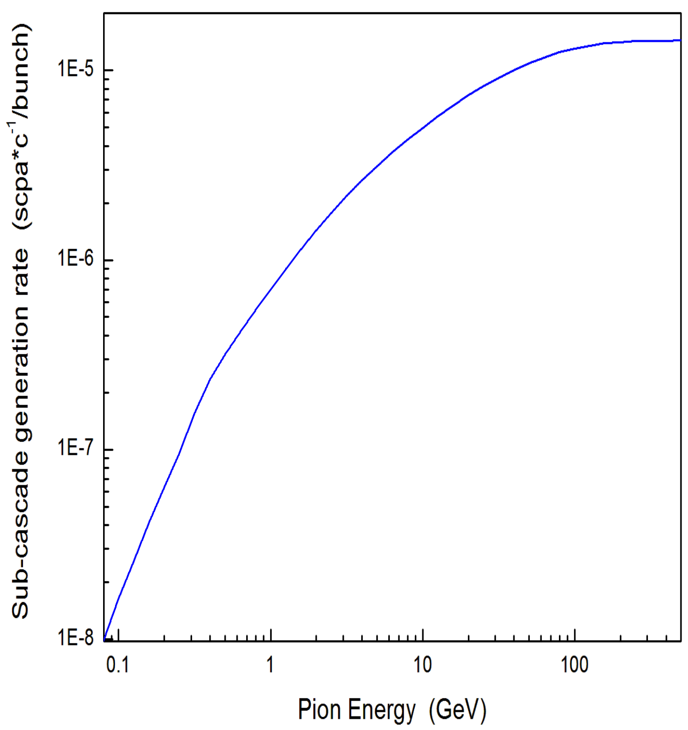

Copper

Sub-cascade generation rate in graphite and copper versus energy of secondary electrons

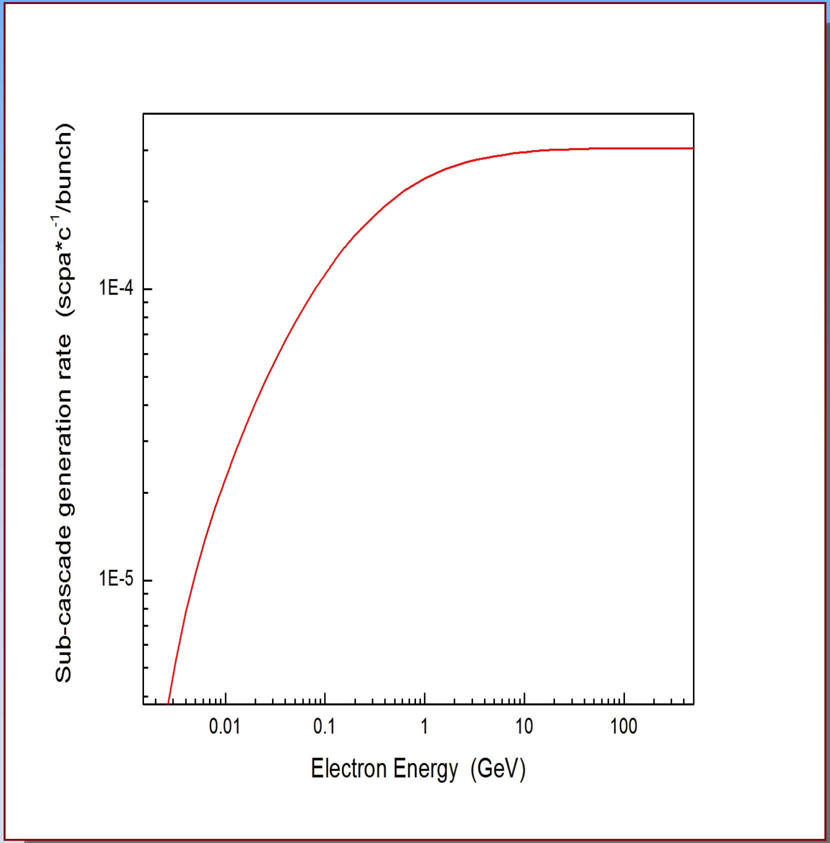

Graphite

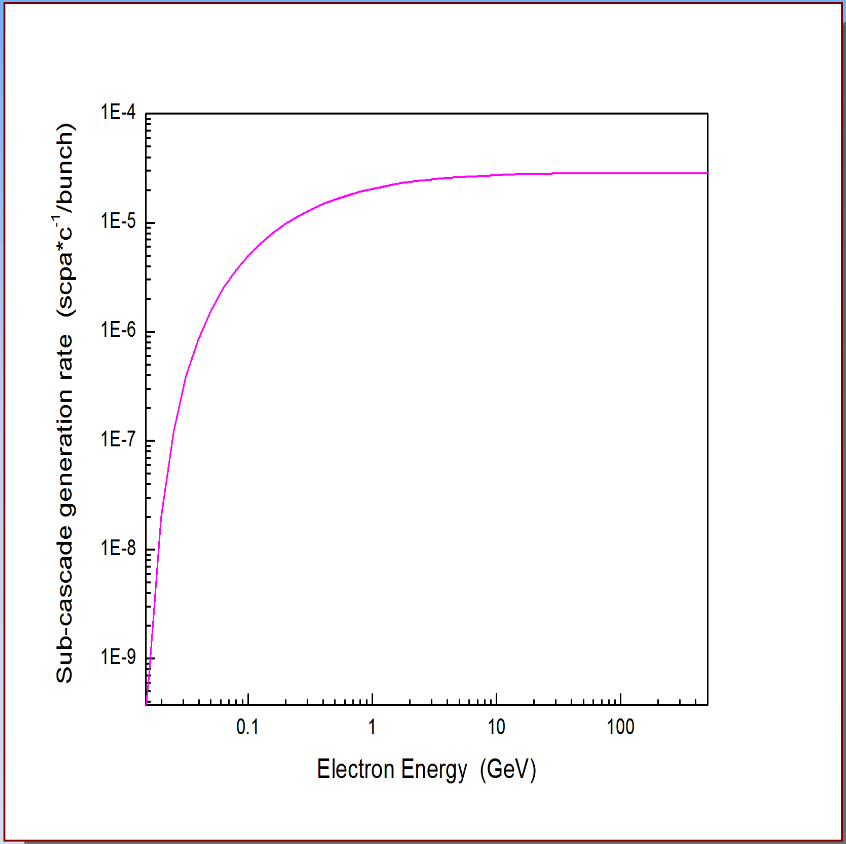

Copper

Theoretical Modeling of Cascade Formation in SiC under Fast Particle Irradiations on NRC KI cyclotron

Sub-cascade space profiles in SiC for fast protons with the energy 10 MeV and fluence 10E17 p/cm2

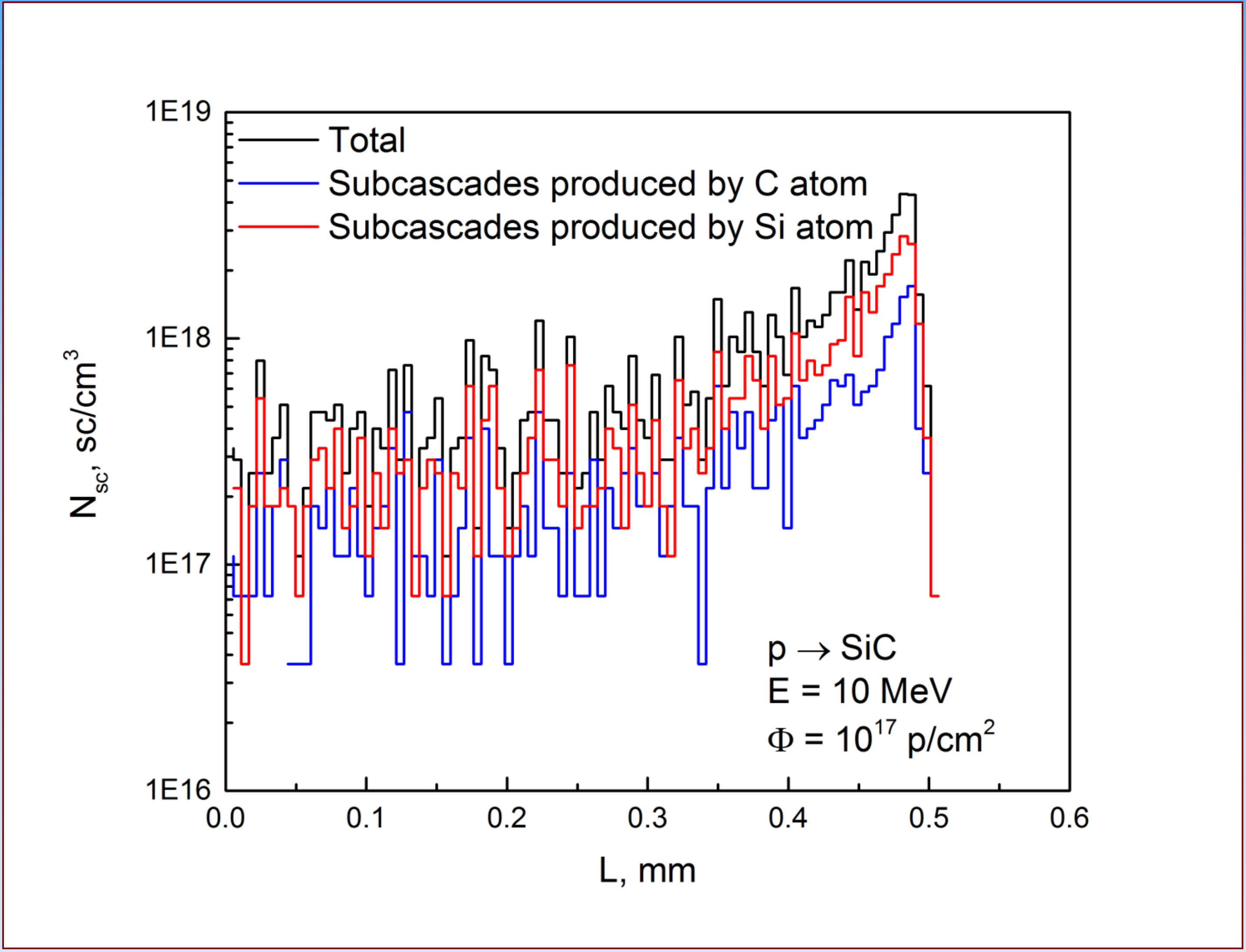

Sub-cascade space profiles in SiC for fast protons with the energy 30 MeV and fluence 10E17 p/cm2

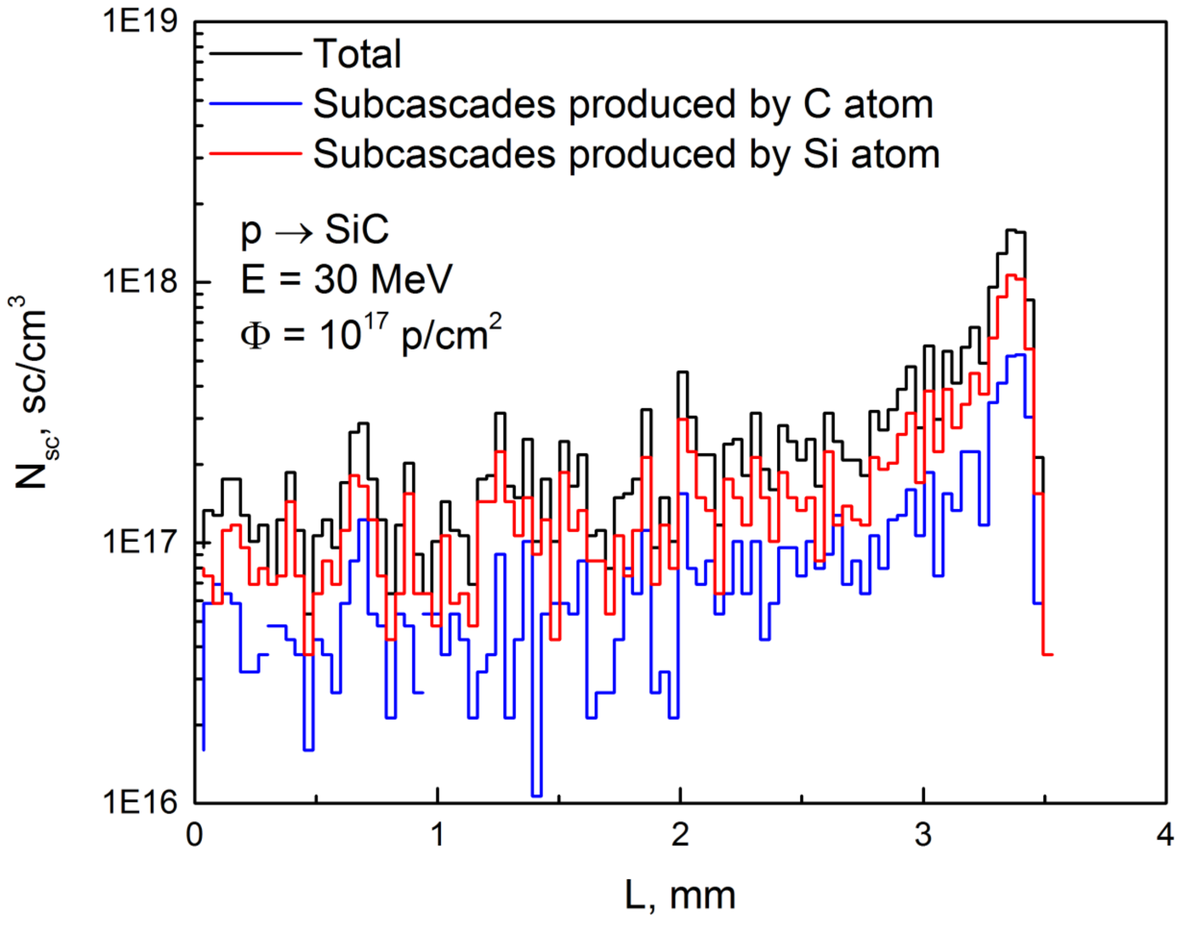

Sub-cascade space profiles in SiC for carbon ion irradiation with the energy 30 MeV and fluence 10E17 p/cm2

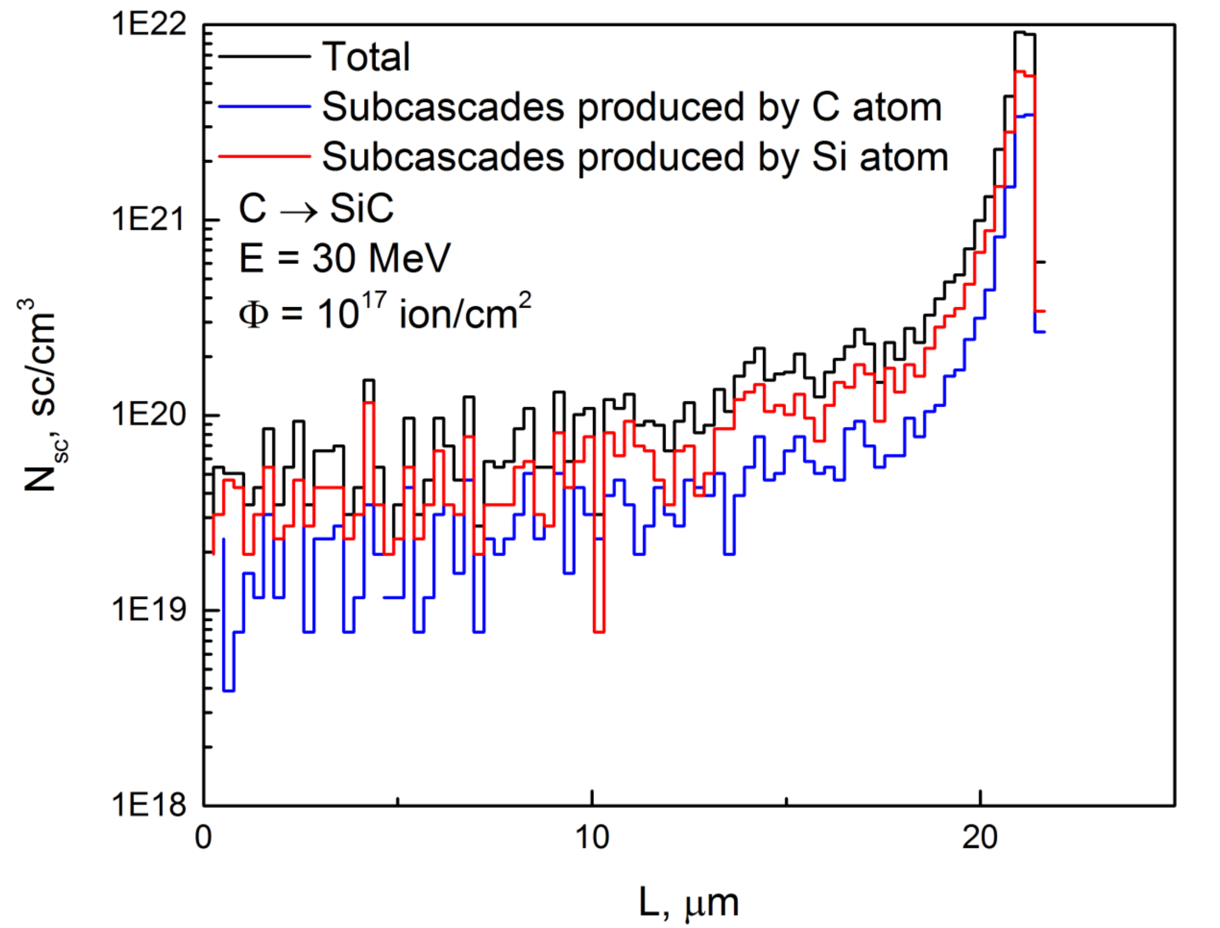

Difference between metals and dielectrics

Metals:

- Point defects are neutral
- Electric field does not exist in the matrix

Dielectrics (Ceramic Materials):

- Point defects can have effective charge
- Electric field exists in the matrix under the influence of an applied electric field
- Driving force due to an electric field can have a strong effect on diffusivity of charged point defects

Theoretical modeling of shock wave formation and radiation damage production in irradiated collimator materials for LHC by protons with energies 450 GeV.

Comparison of the density distributions in Cu after irradiation by 1000 proton bunches with the energy of 450 GeV for two beam sizes 0.3 mm and 5 mm using the free boundary conditions on irradiated material.

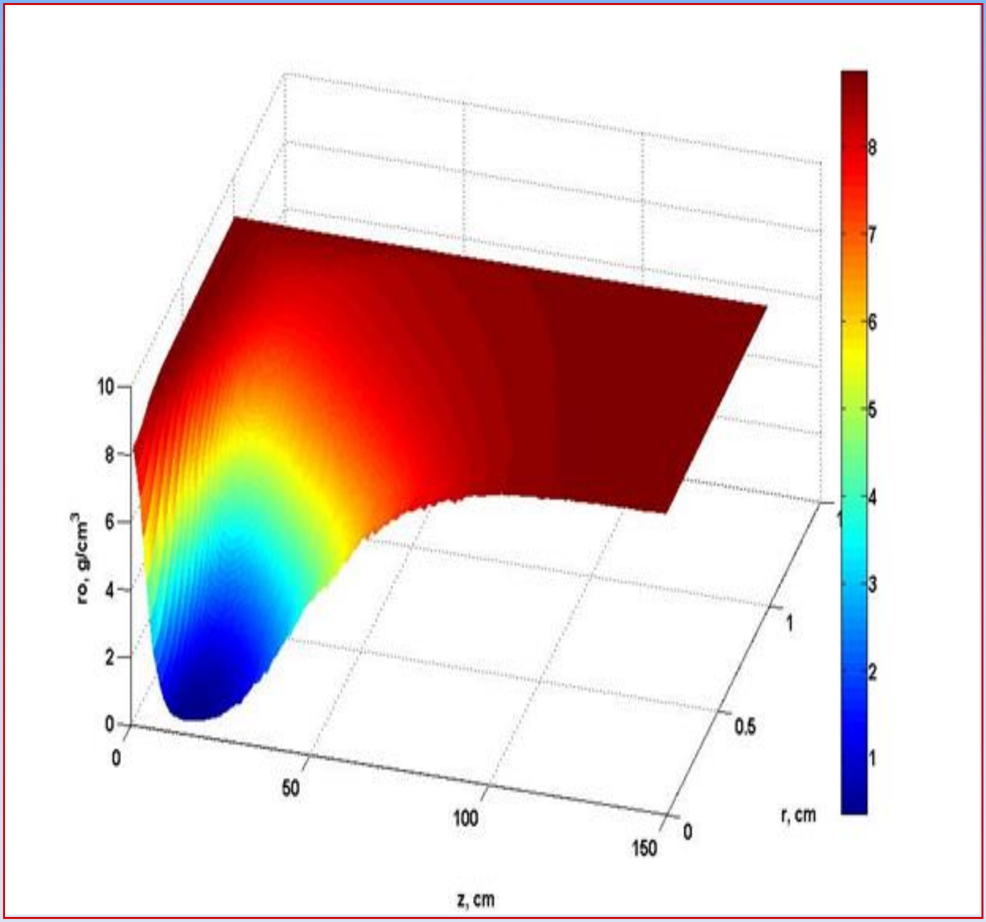

0.3 mm beam size

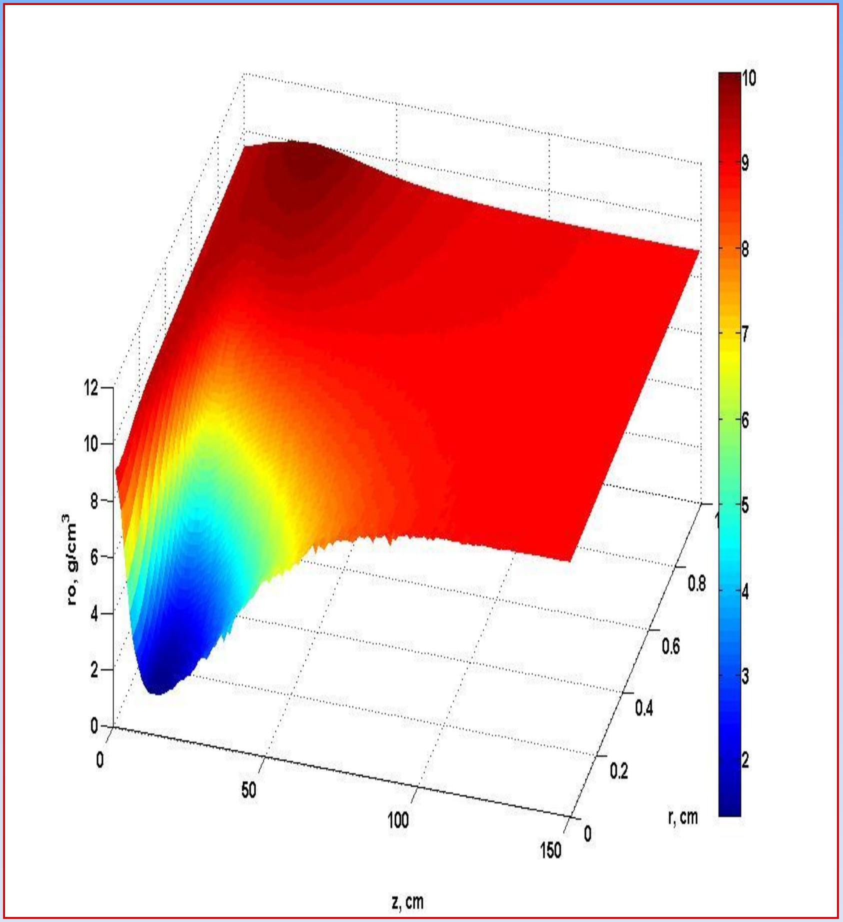

5 mm beam size

Comparison of the temperature distributions in Cu after irradiation by 1000 proton bunches with the energy of 450 GeV for two beam sizes 0.3 mm and 5 mm using the free boundary conditions on irradiated material.

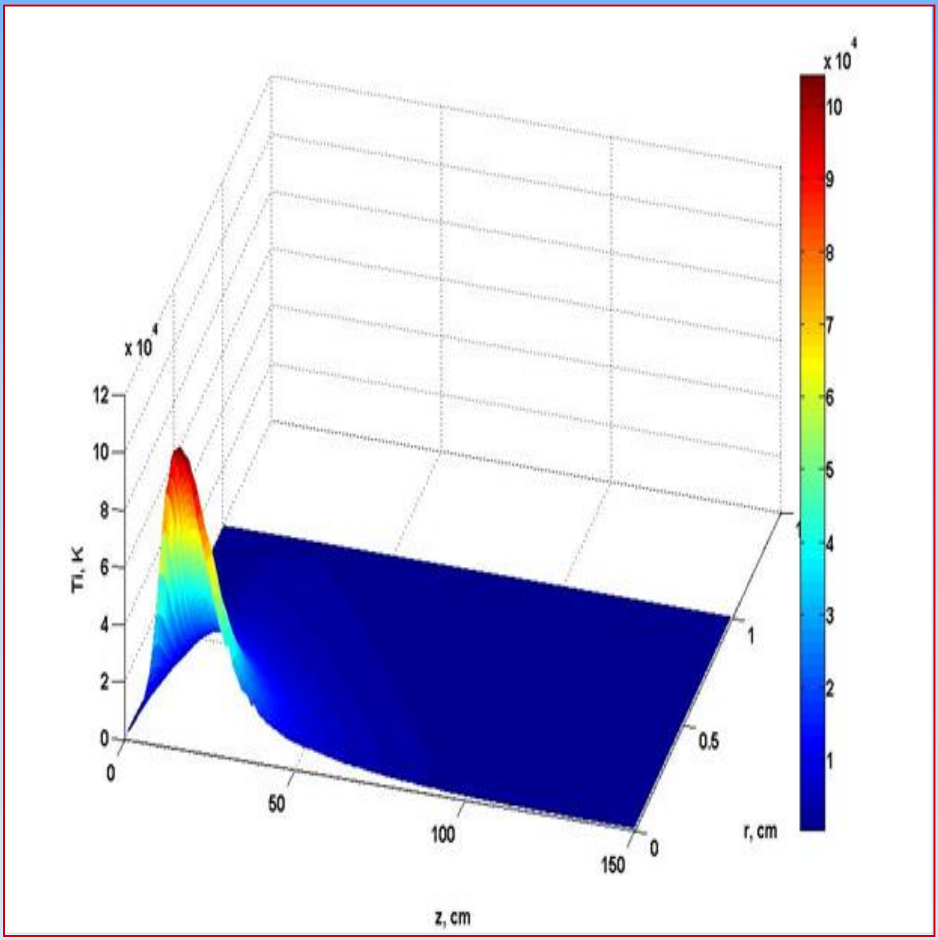

0.3 mm beam size

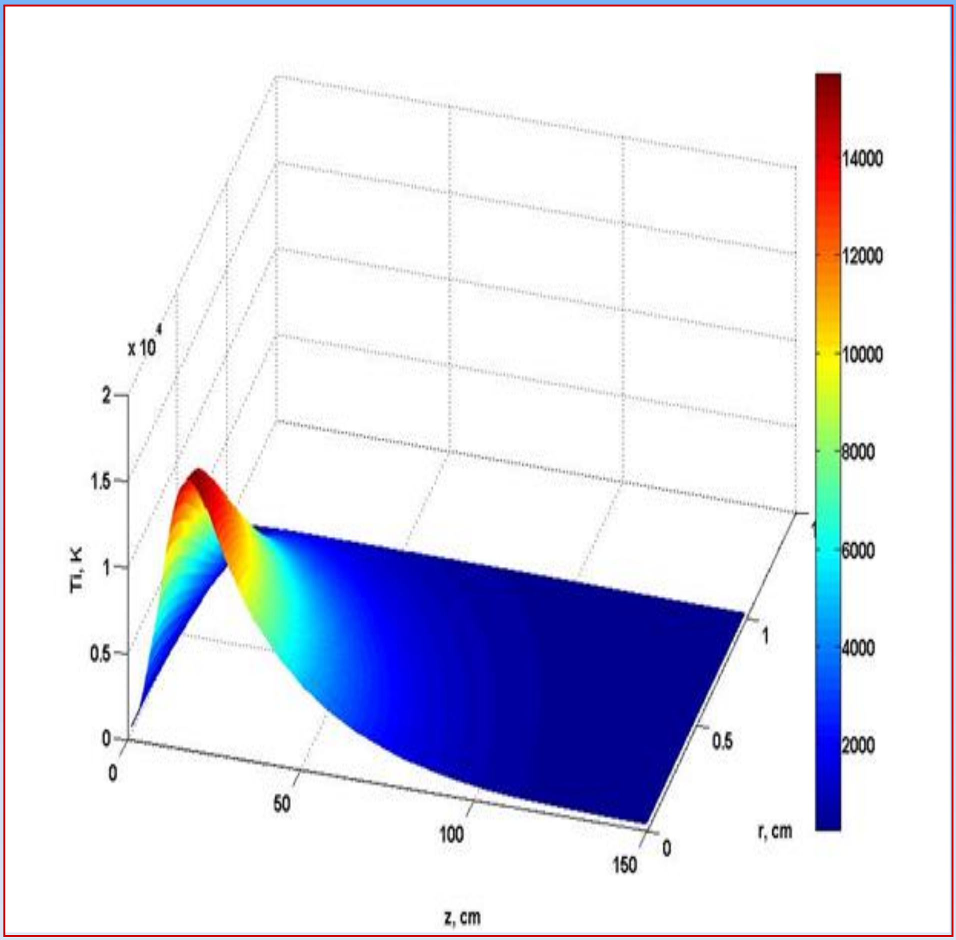

5 mm beam size

Comparison of the internal stress distributions in Cu after irradiation by 1000 proton bunches with the energy of 450 GeV for two beam sizes 0.3 mm and 5 mm using the free boundary conditions on irradiated material.

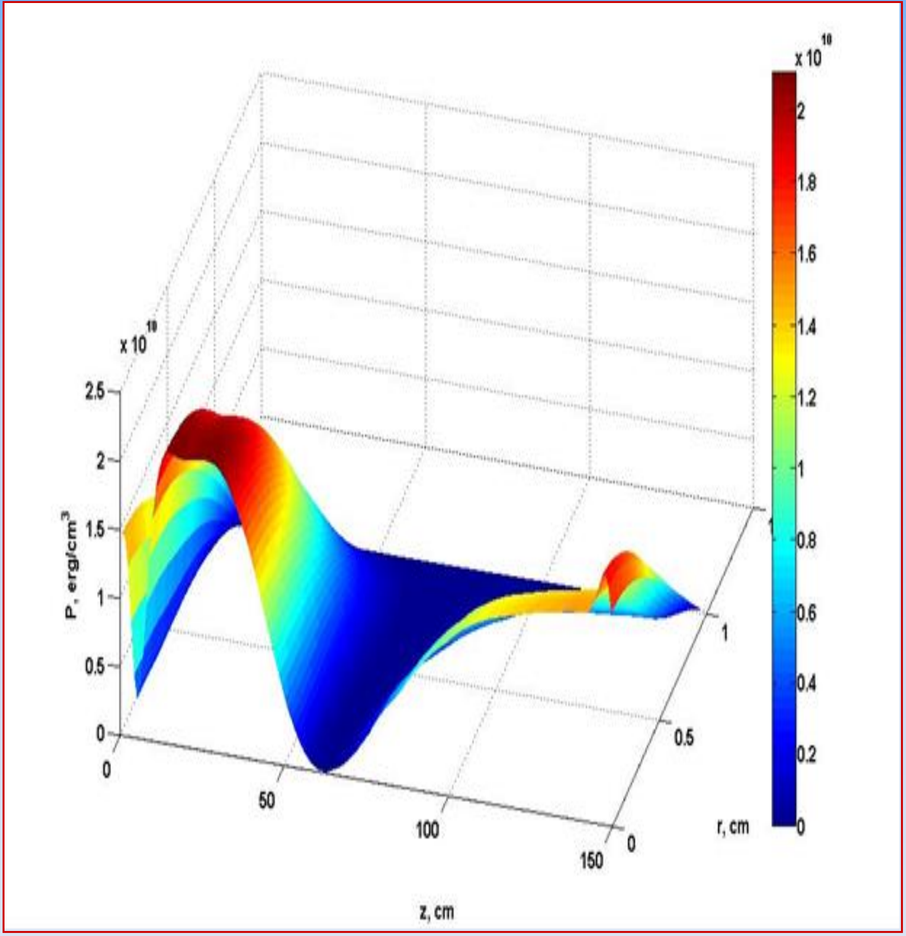

0.3 mm beam size

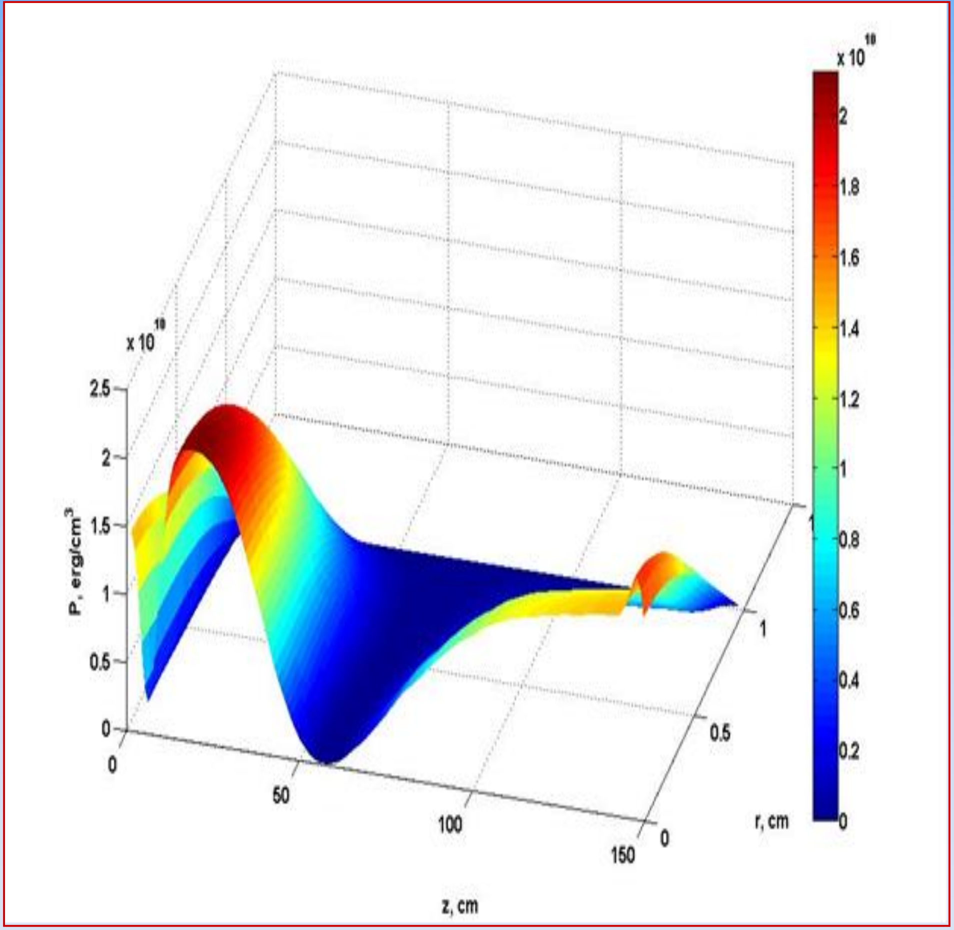

5 mm beam size

Investigations of Mo-Diamond collimator materials before and after 30 MeV proton irradiation on NRC KI cyclotron with dose up to 10E18 1/cm2

Sizes of Mo-Diamond samples used in the investigations

Initial sizes	Mo-Cu-D-1	Mo-Cu-D-2	Mo-Cu-D-3
b, mm	5,68	5,92	5,71
h, mm	4,40	4,50	4,43
S, mm^2	24,96	26,62	25,27
1-st irradiation	Mo-Cu-D-1*	Mo-Cu-D-2*	Mo-Cu-D-3*
b*, mm	5,70	5,95	5,73
h*, mm	4,41	4,51	4,41
S*, mm^2	25,12	26,82	25,26
ΔS/S, %	0,6	0,7	0,0
2-nd irradiation	Mo-Cu-D-1**	Mo-Cu-D-2**	Mo-Cu-D-3**
b**, mm	5,62	5,81	5,65
h**, mm	4,42	4,52	4,42
S**, mm2	24,84	26,29	25,00
ΔS/S, %	-0,5	-1,2	-1,1

Radiation damage profile from protons with energy 30 MeV in MoCuCD material with average density for a dose up to 1017 p/cm2

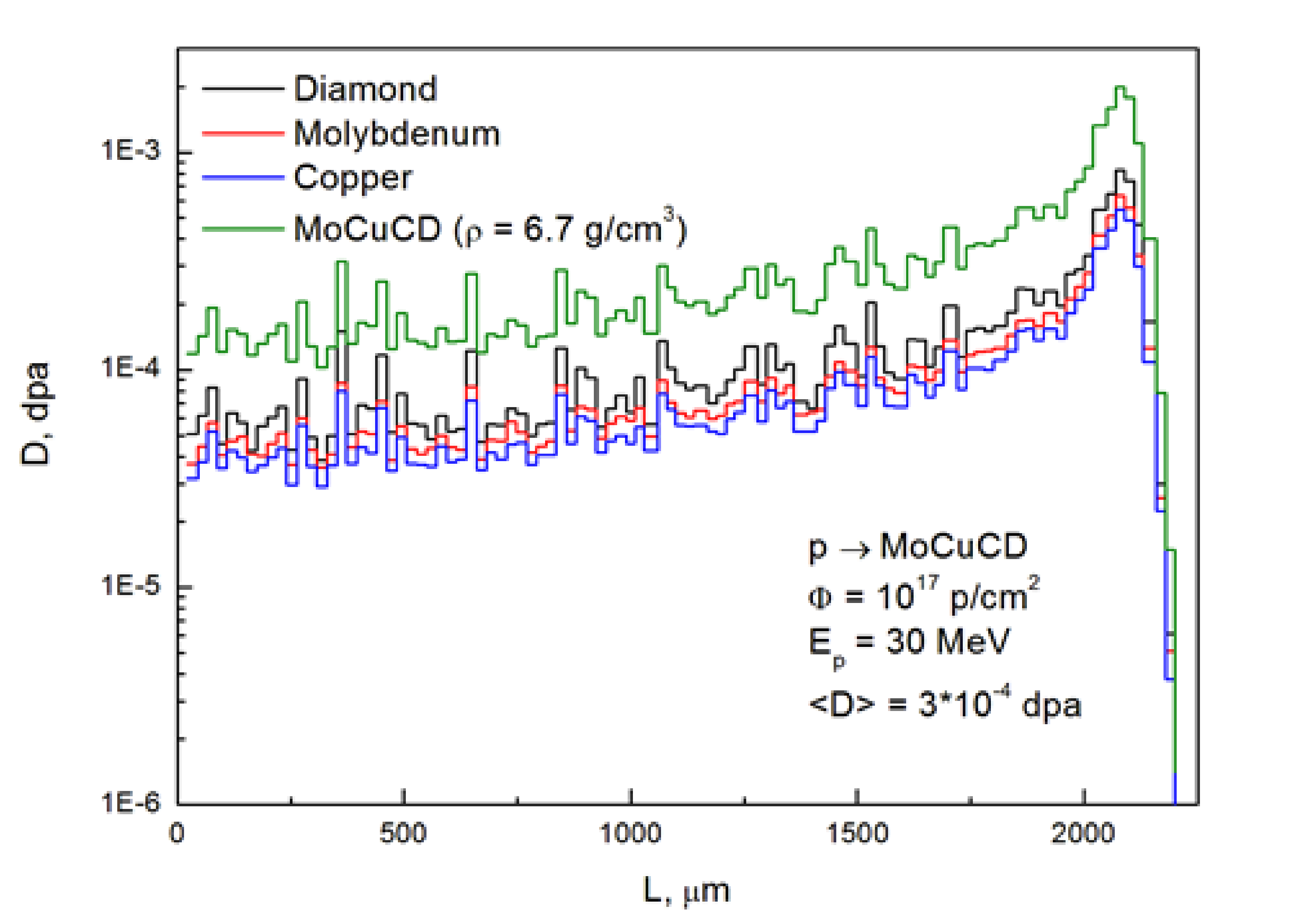

Investigations mechanical properties in Mo-Diamond collimator materials before and after 30 MeV proton beam irradiation on NRC KI cyclotron up to dose 10E18p/cm2

Initial	Mo-Cu-D-1	Mo-Cu-D-2	Mo-Cu-D-3
$F_{M(E)}$, N	100	100	100
σ_E, MPa	34,2	31,2	33,8
$E^И$, GPa	158±8	179±8	155±9
30 MeV, $Ф_1$=10E17 p/cm2	Mo-Cu-D-1*	Mo-Cu-D-2*	Mo-Cu-D-3*
$F_{M(E)}$*, N	50	50	50
σ_E*, MPa	17,1	15,6	16,9
$E^И$*, GPa	184±9	210±9	180±8
$(E^{И*}-E^И)/E^И$, %	16	17	16
30 MeV, $Ф_2$= 10E18 p/cm2	Mo-Cu-D-1**	Mo-Cu-D-2**	Mo-Cu-D-3**
$F_{M(E)}$**, N	50	50	50
σ_E**, MPa	17,1	15,8	17,0
$E^И$**, GPa	200±12	250±10	244±11
$(E^{И**}-E^И)/E^И$, %	26	40	57
$F_{M(\sigma fB)}$**, Н	652,5	945,4	675,9
σ_{fB}**, МПа	222,5	297,8	229,1

Measurements of electrical resistively in Mo-Diamond collimator materials before and after 30 MeV proton beam irradiation on NRC KI cyclotron up to dose 10E18p/cm2

Initial	Mo-Cu-D-1	Mo-Cu-D-2	Mo-Cu-D-3
$\rho_{исх}$, 10^{-6}, Om·m	11,0±0,7	8,5±0,5	9,1±0,5
1-st irradiation E=30 MeV, Φ=10E17 p/cm2	Mo-Cu-D-1*	Mo-Cu-D-2*	Mo-Cu-D-3*
$\rho_{обл}$*, 10^{-6}, Om·m	14±1	11±1	13,7±0,9
($\rho_{обл}$*- $\rho_{исх}$)/$\rho_{исх}$, %	28	29	51
2-nd irradiation E=30 MeV, Φ=10E18 p/cm2	Mo-Cu-D-1**	Mo-Cu-D-2**	Mo-Cu-D-3**
$\rho_{обл}$**, 10^{-6}, Om·m	15±1	11±1	14,1±0,9
($\rho_{обл}$**- $\rho_{исх}$)/$\rho_{исх}$, %	36	29	55

Suggestions for Future Theoretical and Experimental Investigations of Collimator Materials for LHC

1. Development of theoretical models for radiation swelling of different types of collimator materials (graphite, Mo, Cu, SiC, W) after proton irradiations with the energies 450 GeV, 7 TeV in the dependence of number of bunches.
2. Comparison of experimental results for radiation swelling obtained after fast particle irradiation on NRC KI cyclotron and developed theoretical models of radiation swelling of these materials (graphite, Mo, Cu, SiC, W).
3. Investigations of microstructure changes of collimator materials for LHC after proton irradiations with the energies 450 GeV and 7 TeV on Transmission Electron Microscopes of NRC KI.
4. Development of theoretical models for track formation of collimator materials (graphite, Mo, Cu, SiC, W) after heavy ion irradiations with the energies 450 GeV and 7 TeV.